

Taško Maneski¹
Dragan Ignjatović²

SANACIJE I REKONSTRUKCIJE ROTORNIH BAGERA REPAIR AND RECONSTRUCTION OF BUCKET WHEEL EXCAVATORS

Originalni naučni rad / Original scientific paper
UDK /UDC: 620.17:621.879.48
Rad primljen / Paper received: 10.6.2004.

Adresa autora / Author's address:

¹) Mašinski fakultet Univerziteta u Beogradu / Faculty of
Mechanical Engineering, University of Belgrade

²) Rudarsko-geološki fakultet Univerziteta u Beogradu /
Faculty of Mining and Geology, University of Belgrade

UVOD

Izvedene sanacije i rekonstrukcije rotornih bagera su rezultat primene razvijene metodologije dijagnostike čvrstoće konstrukcija; ona podrazumeva proračun kompjuterskim postupkom primenom numeričke metode konačnih elemenata i klasičnog postupka i eksperimentalna merenja. Nalaženje i rešavanje uzroka problema zahteva primenu numeričko-eksperimentalne dijagnostike čvrstoće elemenata. Kompjutersko modeliranje i proračun noseće strukture konstrukcije (KOMIPS) primenjuje numeričku metodu konačnih elemenata kroz statički, dinamički i termički proračun njenih nosećih elemenata.

SANACIJA I REKONSTRUKCIJA RADNOG TOČKA BAGERA C700 O&K (POVRŠINSKI KOP KOLUBARA LAZAREVAC)

Usvojeno opterećenje radnog točka je: obimna sila u iznosu od 232,7 kN i bočna sila u iznosu od 65,9 kN deluju po jednoj kašici. Diskretizovan model radnog točka, prikazan na sl. 1, modeliran je sa 409 linijskih elemenata i 2952 elemenata ploče. Radni točak je u eksploataciji doživeo havariju tako što su vezni limovi točka i vratila popucali. Naponsko polje i raspodele date su na sl. 2.

Rezultati proračuna postojećeg modela nedvosmisleno pokazuju da se najveći napon nalazi tačno na mestu popuštanja konstrukcije točka.

Raspodela normalnih i smicajnih napona ukazuje na veliko prisustvo smicajnih napona. Membranski naponi su dominantni. Analiza pokazuje nedvosmisleno da je uzrok havarije nedovoljna debljina spoljašnje ploče.

Uvođenje kružnog prstena povećane debljine (sa 0,8 mm na 2 cm) na spoljašnjoj ploči donosi znatno smanjenje napona u spoljašnjoj ploči (napon je smanjen sa 21,6 kN/cm² na 13,6 kN/cm²) uz značajno smanjenje učešća smicajnog napona. Točak uspešno radi.

INTRODUCTION

Performed repair and reconstruction of bucket wheel excavators is the result of applied developed methodology of structural diagnostics; it includes computer based calculation by numerical finite element method and classic engineering procedure, and experimental measurements. Finding and solving the problem causes require the use of numerical and experimental diagnostics of element strength. Computer modelling and calculation of supporting structures (KOMIPS) uses the finite element method through static, dynamic, and thermal calculations of its supporting elements.

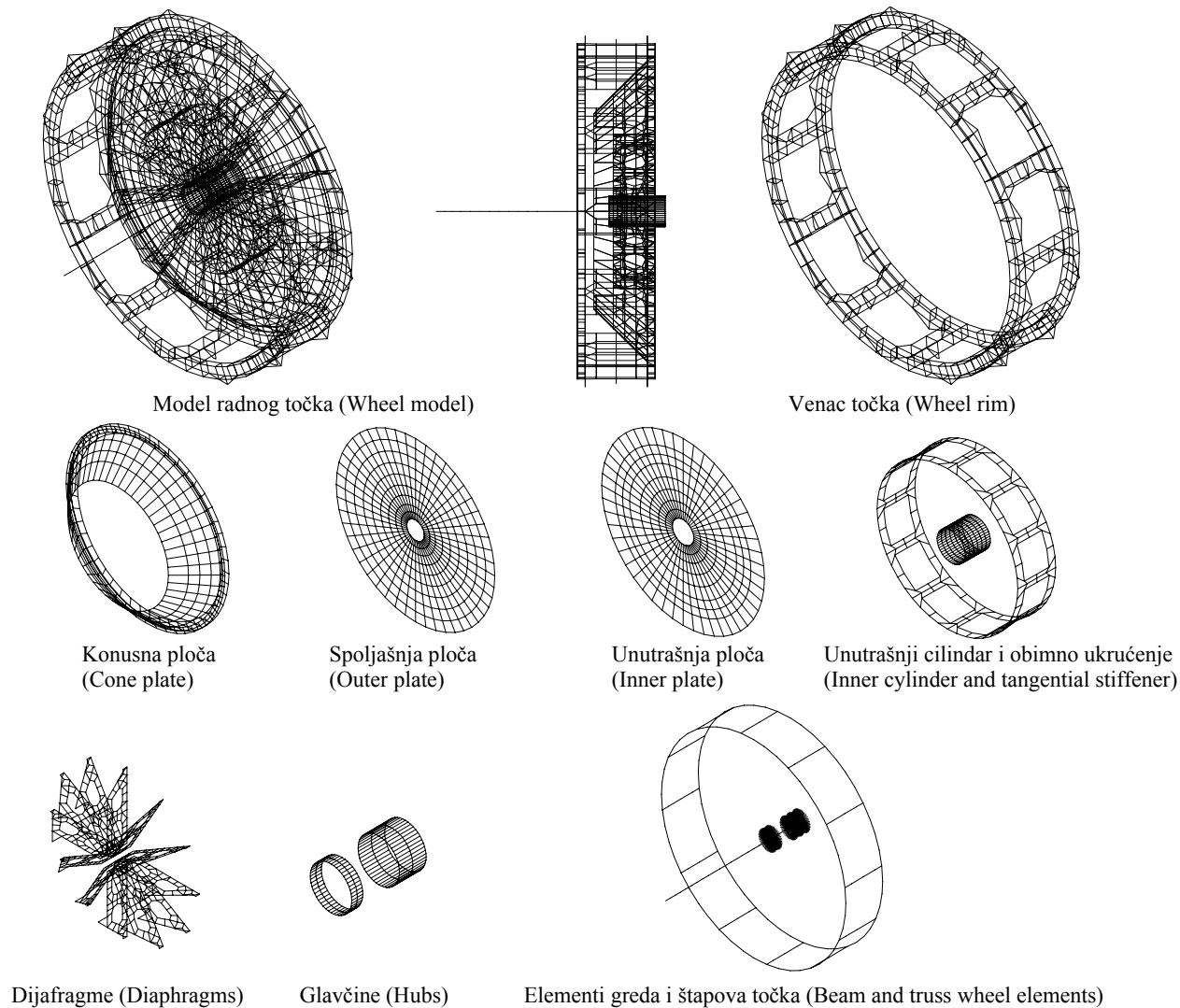
REPAIR AND RECONSTRUCTION OF OPERATING WHEEL ON EXCAVATOR C700 O&K (OPEN-CAST MINE KOLUBARA LAZAREVAC)

The following operating wheel loads are approved: circumferential force 232.7 kN; lateral force 65.9 kN, per bucket. The discretized operating wheel model, shown in Fig. 1, consists of 409 linear elements and 2952 plate elements. The operating wheel failed in service, causing cracking of connected plates and shafts. The stress fields and distributions are shown in Fig. 2.

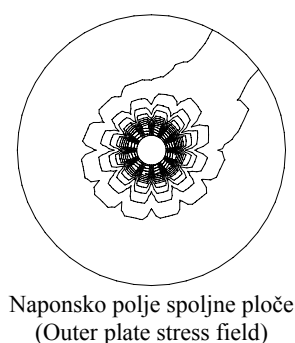
Numerical results of the existing model clearly point out that the largest stress is located at the position of yielding of the operating wheel.

The distribution of normal and shear stresses indicates large presence of shear stresses. Membrane stresses are dominant. The analysis undoubtedly shows that the failure is caused by insufficient thickness of the outer plate.

Adding a ring of increased thickness (2 cm instead of 0.8 cm) to the outer plate led to significant stress decrease (from 21.6 to 13.6 kN/cm²) and also to a decrease in the shear stress effect. The wheel has continued to operate successfully.



Slika 1. Modeli radnog točka i podstruktura
Figure 1. Wheel models and substructures.



Naponsko polje spoljne ploče
(Outer plate stress field)

Napon (Stress) [kN/cm ²], Raspodela (Distribution) [%]		
	Postojeći model Existing model	Saniran model Repaired model
Usrednjen σ_{max}^{ekv} tačke venca Average σ_{max}^{eq} – rim points	12.1	12.2
Usrednjen σ_{max}^{ekv} tačke/elementa spolj. ploče Average σ_{max}^{ekv} – outer plate	14.4/21.6	9.1/13.6
Raspodela membranski/savojni napon Membrane/bending stress distribution	84.1/15.9	85/15
Raspodela normalni/smicajni napon Normal/shear stress distribution	43.6/56.4	50/50

Slika 2. Naponsko polje i raspodele
Figure 2. Stress state and the distributions.

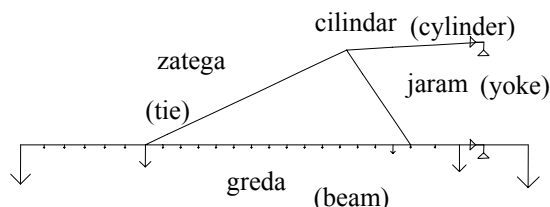
REKONSTRUKCIJA STRELE ROTORNOG BAGERA C700 O&K (POVRŠINSKI KOP KOLUBARA)

U eksploataciji bagera često dolazi do veoma lošeg dinamičkog ponašanja odložne strele, tj. ona ulazi u rezonancu pri čemu amplitude oscilovanja dostižu 60 cm. Ponekad dolazi do pucanja elementa odložne trake. Konstrukcija je sastavljena od jednog grednog elementa i tri štapa (zatega,

BEAM RECONSTRUCTION OF B/W EXCAVATOR C700O&K (OPEN-CAST MINE KOLUBARA)

During excavator service life, poor dynamic behaviour of the unloading beam is frequent, i.e. with resonant oscillations, amplitudes up to 60 cm. This may result in cracking of certain cantilever elements. The structure consists of one beam element and three truss elements (tie, yoke and cylinder).

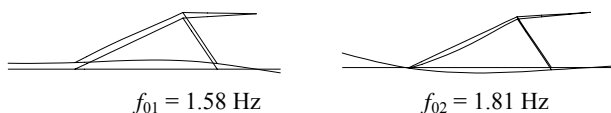
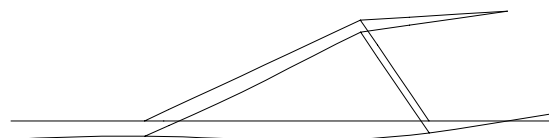
jaram i cilindar). Na sl. 3. prikazan je model i deformacija strele. Raspodela energije deformisanja je: greda (72,2%); zatega (16,8%); cilindar (10,5%) i jaram (0,5%). Zaključak statičkog proračuna glasi: veliki nagib grede u zglobnom osloncu; podužna sila je velika u zatezi i cilindru, dok je u jarmu mala; moment savijanja grede je veliki na mestu veze sa jarmom; energija deformisanja grede je dominantna.



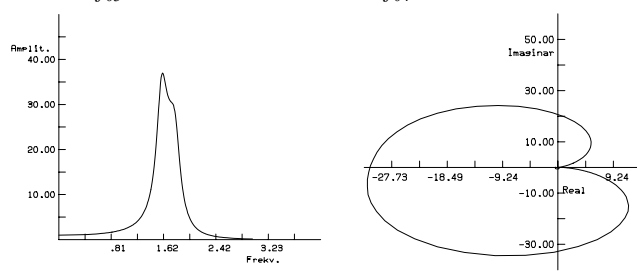
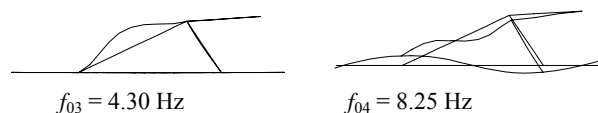
Slika 3. Ravanski model strele i deformacija strele ($f_{max} = 10.4$ cm)
 Figure 3. Planar model of the cantilever beam and deformation pattern ($f_{max} = 10.4$ cm).

Zaključak dinamičkog proračuna (sl. 4): prve dve frekvencije su veoma niske i bliske, poklapaju se sa statičkom deformacijom; faktor dinamičkog pojačanja je vrlo velik; velik je imaginarni deo karakteristike (nestabilan sistem) i energije su dominantne na gredi i na spoljašnjim masama.

Figure 3 shows the cantilever model and strain pattern. Strain energy is distributed as follows: beam (72.2%); tie (16.8%); cylinder (10.5%); yoke (0.5%). Static calculation has concluded: too large tilting of the beam in the support joint; the axial force in tie and cylinder is too large, but rather low in the yoke; the bending moment of the beam is large in yoke link; and dominant strain energy in beam.



Raspodele [%], elementi strukture (Distribution [%], structural elements)	Potencijalna/Kinetička energija (Potential/Kinetic energy)	
	$f_{01} = 1.58$ Hz	$f_{02} = 1.81$ Hz
Greda (Beam)	80/35	90/16
Zatega (Tie)	12/3	6/1
Cilindar (Cylinder)	8/0	4/0
Jaram (Yoke)	0/0	0/0
Spolj. mase (Ext. mass)	62	73



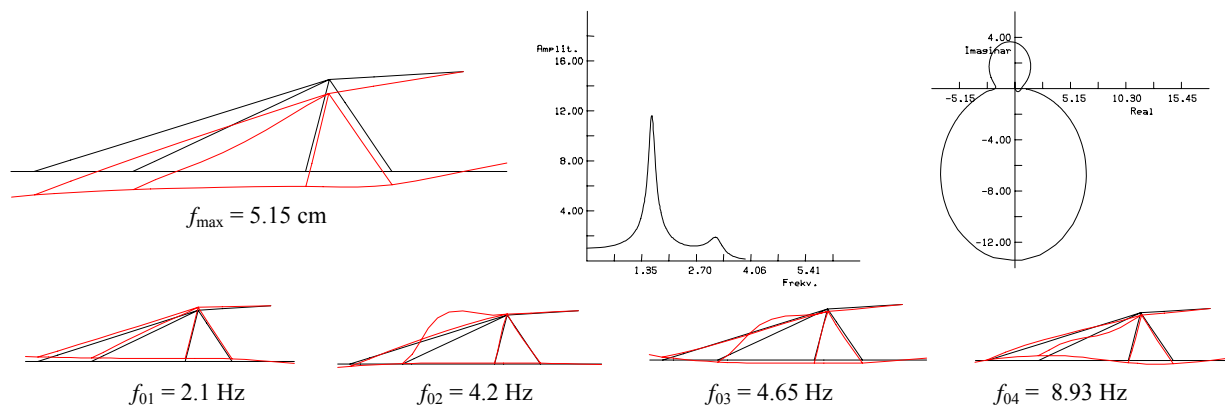
Slika 4. Prva četiri glavna oblika oscilovanja, raspodele i jedan frekventni odziv
 Figure 4. First four major forms of oscillation, distribution, and one frequency response.



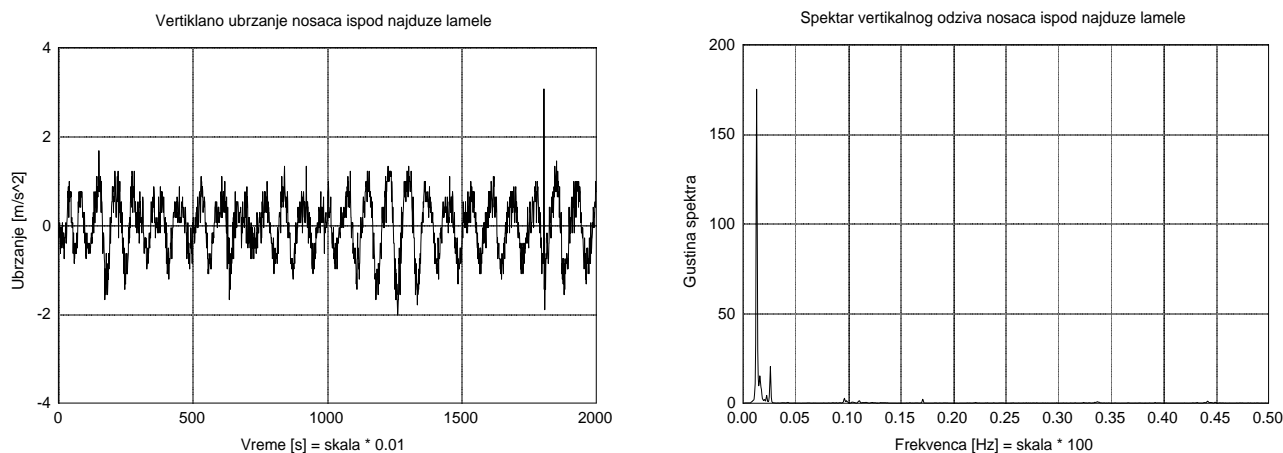
Slika 5. Rekonstrukcija strele
 Figure 5. Cantilever beam reconstruction.

Rekonstrukcija strele se odnosi na uvođenje dve nove zatege, pojačanje jarma strele i uklanjanje teške kućice (uvedene su kamere) (sl. 5). Model i rezultati proračuna prikazani su na sl. 6. Strela uspešno radi. Na rekonstruisanoj strelji izvršeno je merenje ubrzanja na zategama i gredi. Na sl. 8 prikazan je jedan izmereni signal. Vidi se da je ubrzanje ispod dozvoljene vrednosti (2 m/s^2) i nema odziva na sopstvenoj frekvenciji strele.

Cantilever reconstruction meant adding two new ties, yoke reinforcement and removal of heavy elements (cameras were placed) (Fig. 5). Numerical results and model are shown in Fig. 6. The cantilever operates successfully. Acceleration measurements were made on the reconstructed beam and ties. Figure 8 shows a measured signal. As can be seen, the acceleration is below the allowed value (2 m/s^2) and with no response of cantilever eigen-frequency.



Slika 6. Rezultati statičkog i dinamičkog proračuna rekonstruisane strele
Figure 6. Static and dynamic numerical results of the reconstructed cantilever.



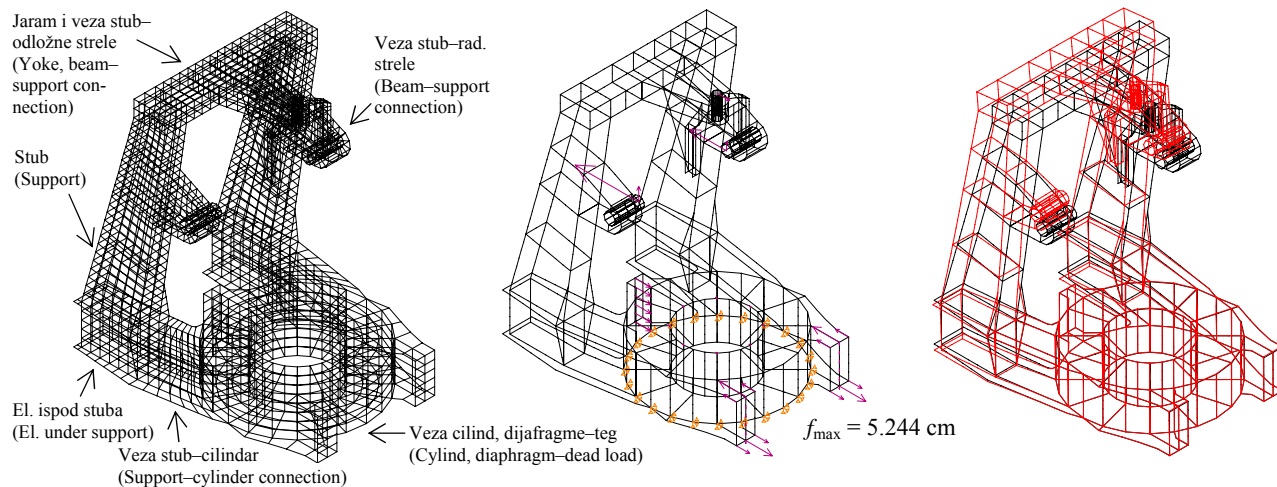
Slika 7. Vertikalno ubrzanje u vremenskom (levo) i gustina spektra u frekventnom domenu (desno)
Figure 7. Vertical acceleration in time (left) and spectrum density in frequency domain (right).

SANACIJA I REKONSTRUKCIJA GORNJE GRADNJE BAGERA C700 O&K (POVRŠINSKI KOP KOLUBARA)

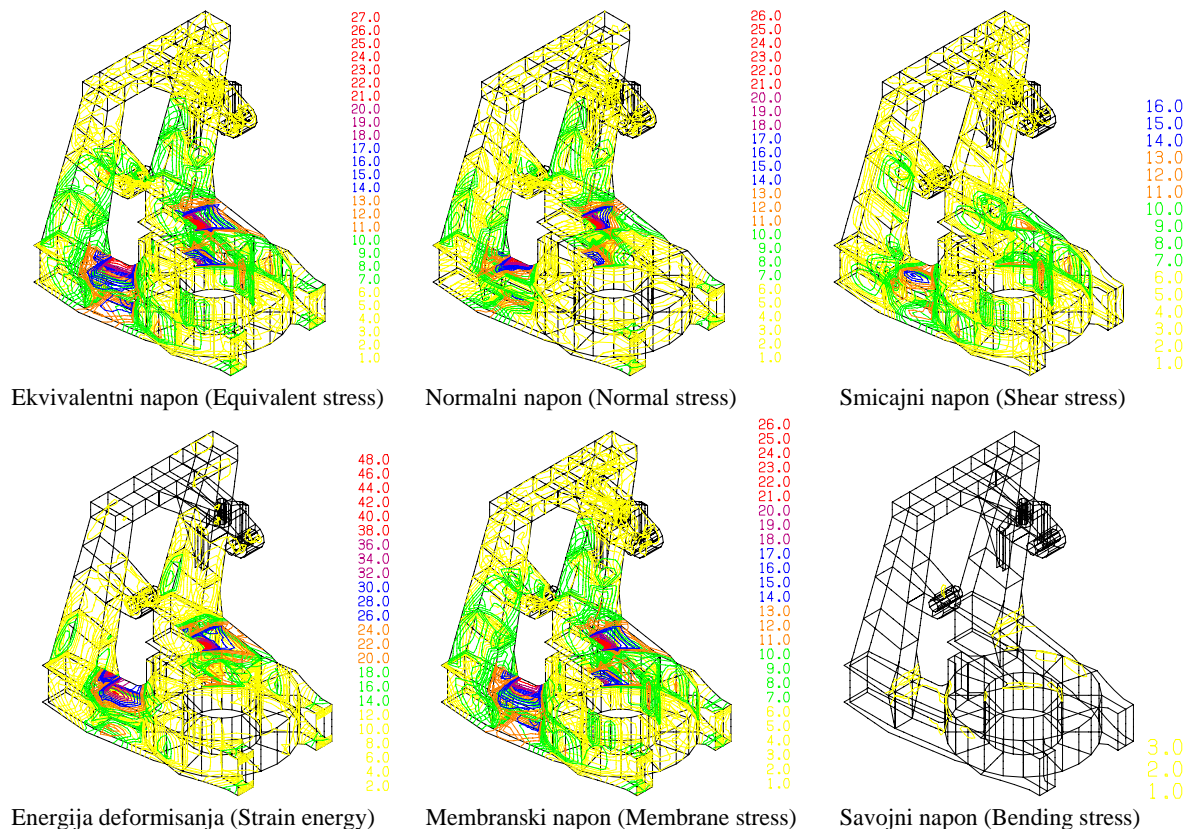
REPAIR AND RECONSTRUCTION OF UPPER EXCAVATOR C700O&K (OPEN-CAST MINE KOLUBARA)

Ova analiza ima za cilj da otkrije uzroke pucanja veze stuba i cilindra, lošeg ponašanja gornje gradnje i da ih eliminiše. Računski model gornje gradnje bagera, najnepovoljnije opterećenje i deformacija prikazani su na sl. 8. Elementi dijagnostike čvrstoće gornje gradnje i detaljnija analiza ponašanja donje gradnje dati su u nastavku.

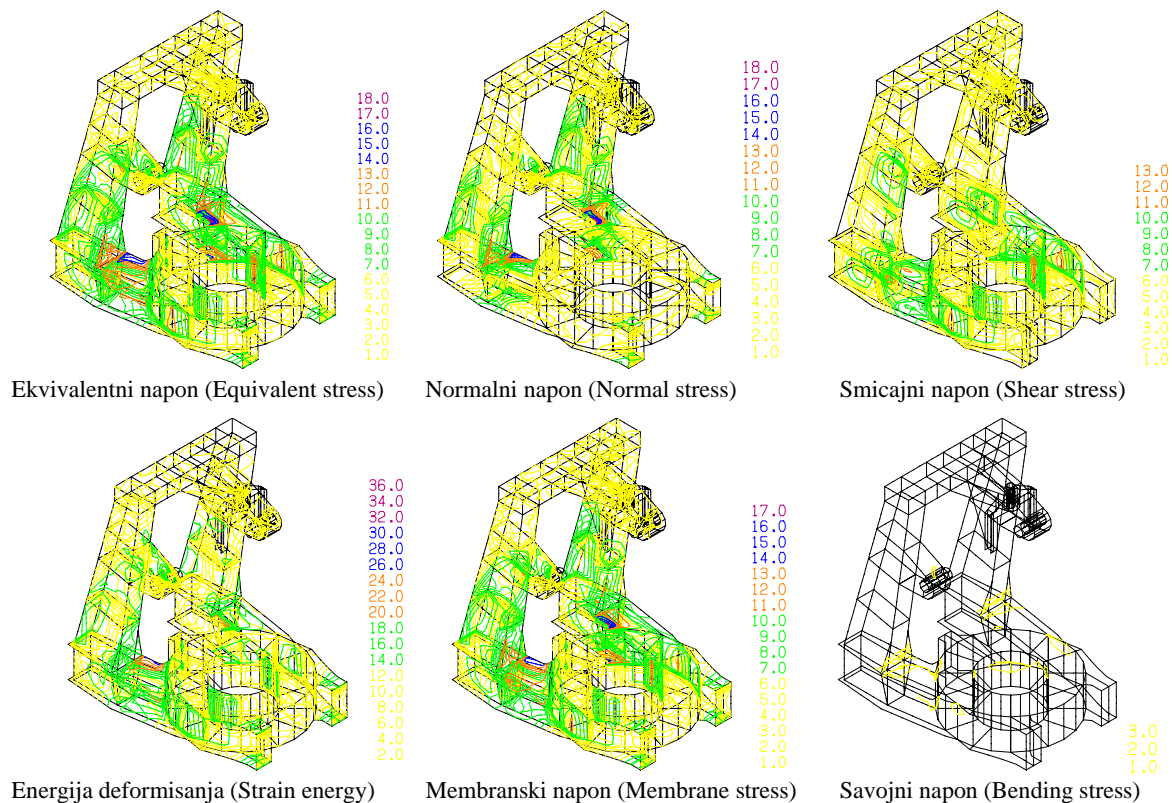
The analysis is aimed in determining and resolving cracking causes of support and cylinder connection and poor dynamic behaviour of upper assembly. Upper assembly numerical model and strain pattern with worst loading case are shown (Fig. 8). Upper element strength diagnostics and detailed analysis of lower assembly behaviour are shown below.



Slika 8. Računski model gornje gradnje bagera sa najnepovoljnijim opterećenjem i deformacijom
Figure 8. Numerical model of upper excavator assembly with worst case load and deformation.



Slika 9. Raspodela napona [kN/cm²] i energije deformisanja [kNcm]
 Figure 9. Stress [kN/cm²] and strain energy [kNcm] distribution.



Slika 10. Raspodela napona [kN/cm²] i energije deformisanja [kNcm] rekonstruisane gornje gradnje
 Figure 10. Stress [kN/cm²] and strain energy [kNcm] distribution of reconstructed upper assembly.

Tabela 1. Analiza ponašanja gornje gradnje - Table 1 Analysis of upper assembly behaviour.

Raspodela (Distribution) [%]	$\sigma_{\max}^{\text{ekv}}$ [kN/cm ²]	σ/τ	mem./sav mem/bend	E_d relativ./absol
Stub (Support)	14	17.1/15.7	31.3/1.3	24.6/27.3
Elem. ispod stuba (Elem. beneath the support)	16	6.0/6.2	11.6/0.4	16.1/10.9
Elem. veze stub–cilindar (Elem. of support–cylinder connection)	27.3	12.7/9.4	20.4/1.2	34.3/39.3
Elem. veze stub–radna strela (Elem. of support–load beam conn.)	9	3.8/1.6	5.0/0.5	1.9/3.6
Jaram i elem. veze stub–odl. strela (Yoke and support–unload beam)	6	3.8/3.5	6.7/0.6	1.6/2.5
Cilin., dijafragme i elem. kontra tega (Cyl., diaphragm and dead load)	13	6.3/13.8	19.5/1.5	21.5/16.4
Suma (Total)		49.7/50.3	94.5/5.5	6637 [kNcm]

Zaključak analize glasi:

- najveći napon, koncentraciju i energiju deformisanja imaju elementi veze stuba i cilindra,
- stub i cilindri imaju nizak nivo napona na velikoj površini uz visok udeo u naponu i energiji,
- jaram ima najmanji uticaj na ponašanje.

Loše ponašanje gornje gradnje možemo popraviti povećanjem debljine gornje i donje horizontalne ploče elementa veze stuba i cilindra. Usvojeno povećanje debljine gornje ploče je za 15 mm, odnosno ukupno 39 mm, dok donje za 10 mm (ukupno 34 mm). Maksimalna deformacija je sada $f_{\max} = 4,669$ cm. Sledi prikaz elemenata dijagnostike čvrstoće rekonstruisane gornje gradnje (sl. 10), dok je na sl. 11. prikazana izvedena rekonstrukcija.

From this analysis we conclude the following:

- support–cylinder connecting elements have the largest stress, stress concentration, and strain energy,
- support and cylinders have a low stress level on a large surface with a high contribution of stress and energy,
- the yoke has the least significant effect on the behaviour.

Inproper upper assembly behaviour can be corrected by increasing thickness of upper and lower horizontal plate connecting elements. An upper plate thickness increase of 15 mm, i.e. a total of 39 mm was approved, while lower plate thickness was increased 10 mm (34 mm total). The maximum strain value is now $f_{\max} = 4.669$ cm. Figure 10 shows strength diagnostics of reconstructed upper assembly elements, and Fig. 11 shows the reconstructed assembly.



Slika 11. Izvedena sanacija i rekonstrukcija gornje gradnje
Figure 11. Performed repair and reconstruction of upper assembly.

Uvođenje novih vertikalnih ploča dovodi do značajnog poboljšanja ponašanja donje gradnje kroz:

- smanjenje maksimalne deformacije za 10,96%,
- smanjenje maksimalnog napona za 34%,
- smanjenje energije deformisanja za 10,3%,
- nivoi koncentracije napona i energije deformisanja su značajno smanjeni.

Izvedeni proračun i analiza nedvosmisleno ukazuju na potrebu povećanja debljine horizontalnih ploča.

SANACIJA I REKONSTRUKCIJA DONJE GRADNJE BAGERA C700 O&K (POVRŠINSKI KOP KOLUBARA LAZAREVAC)

Konstrukcija donje gradnje bagera pretrpela je u više navrata delimična i potpuna pucanja veznih nosača donje gradnje i transportnog bagera (sl. 12). Računski model i rezultati proračuna dati su na sl. 13. i 14. Analiza starog i novog rešenja data je u tabeli 2.

Introduction of new vertical plates led to significant improvements in the behaviour of the lower assembly, such as:

- maximum strain decrease for 10.96%,
- maximum stress decrease for 34%,
- strain energy decrease for 10.3%,
- significant decrease in levels of stress concentration and strain energy.

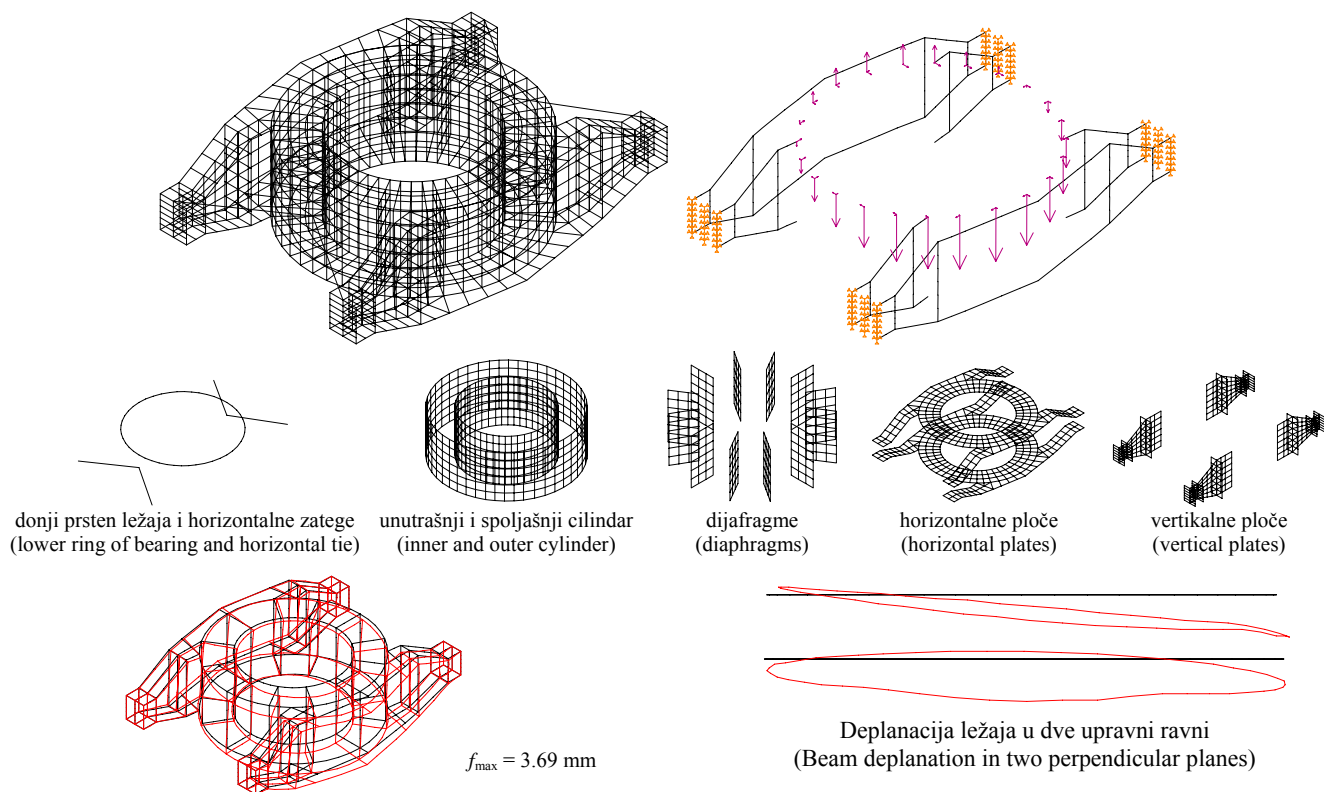
The calculation and analysis clearly point out the need for increasing the thickness of horizontal plates.

REPAIR AND RECONSTRUCTION OF EXCAVATOR LOWER ASSEMBLY, C700 O&K (OPEN-CAST MINE KOLUBARA LAZAREVAC)

The excavator lower assembly suffered several partial and complete cracking of assembly connection beams (see Fig. 12). Model and numerical results are shown in Fig. 13 and 14. Table 2 shows the analysis of the old and new solution.



Slika 12. Oštećenja veznih nosača donje gradnje transportnog bagera
Figure 12. Damaged connection beams in the excavator lower assembly.



Slika 13. Računski model i deformacija
Figure 13. Computational model and deformation.

Tabela 2. Analiza ponašanja stare i nove gornje gradnje - Table 2. Old and new upper assembly behaviour analysis.

Raspodela [%] (Distribution)	$\sigma_{\max}^{\text{ekv}}$ [kN/cm ²]		σ/τ		mem./sav		mem/bend		E_d relativ./apsol.	
	Staro (Old)	Novo (New)	Staro (Old)	Novo (New)	Staro (Old)	Novo (New)	Staro (Old)	Novo (New)	Staro (Old)	Novo (New)
Cilindri (Cylinders)	7	6.3	28.8/19.2	24/15.5	38.2/9.8	31.4/8.4	26/29.9	31.9/29		
Dijafragme (Diaphragms)	7	4.6	3.2/1.8	2.4/1.5	4.1/0.9	3.2/0.7	0.9/1.3	1/1.2		
Horiz.ploče (Horizontal plates)	11	7	14.8/4	10/2.2	15/3.9	9.7/2.6	20.3/17.2	16.8/10.7		
Vertikalne ploče (Vertical plates)	12.9	6.4	12/15.1	7.5/8.2	23.9/3.3	13.9/1.8	49.3/50.8	25.9/20.9		
Linijski elem. (Linear elem.)	-	-	0.9/0.2	0.7/0.2	0.9/0	0.7/0	3/0.7	4.2/0.6		
Novo vert.plo. (New vert. plates)	-	7.44	-	14.3/13.2	-	24 / 3.6	-	20.2/37.6		
Suma (Total)			59.7/40.3	59.2/40.8	82/18	82.9/17.1	1200	910 [kNcm]		

Zaključak analize glasi:

- najveći napon i energiju deformacije imaju vertikalne ploče,
- na horizontalnim pločama je velik napon na maloj površini,
- cilindri imaju nizak nivo napona na velikoj površini uz visok procentualni udeo u naponu i energiji,
- dijafragme imaju najmanji uticaj na ponašanje.

This analysis has concluded the following:

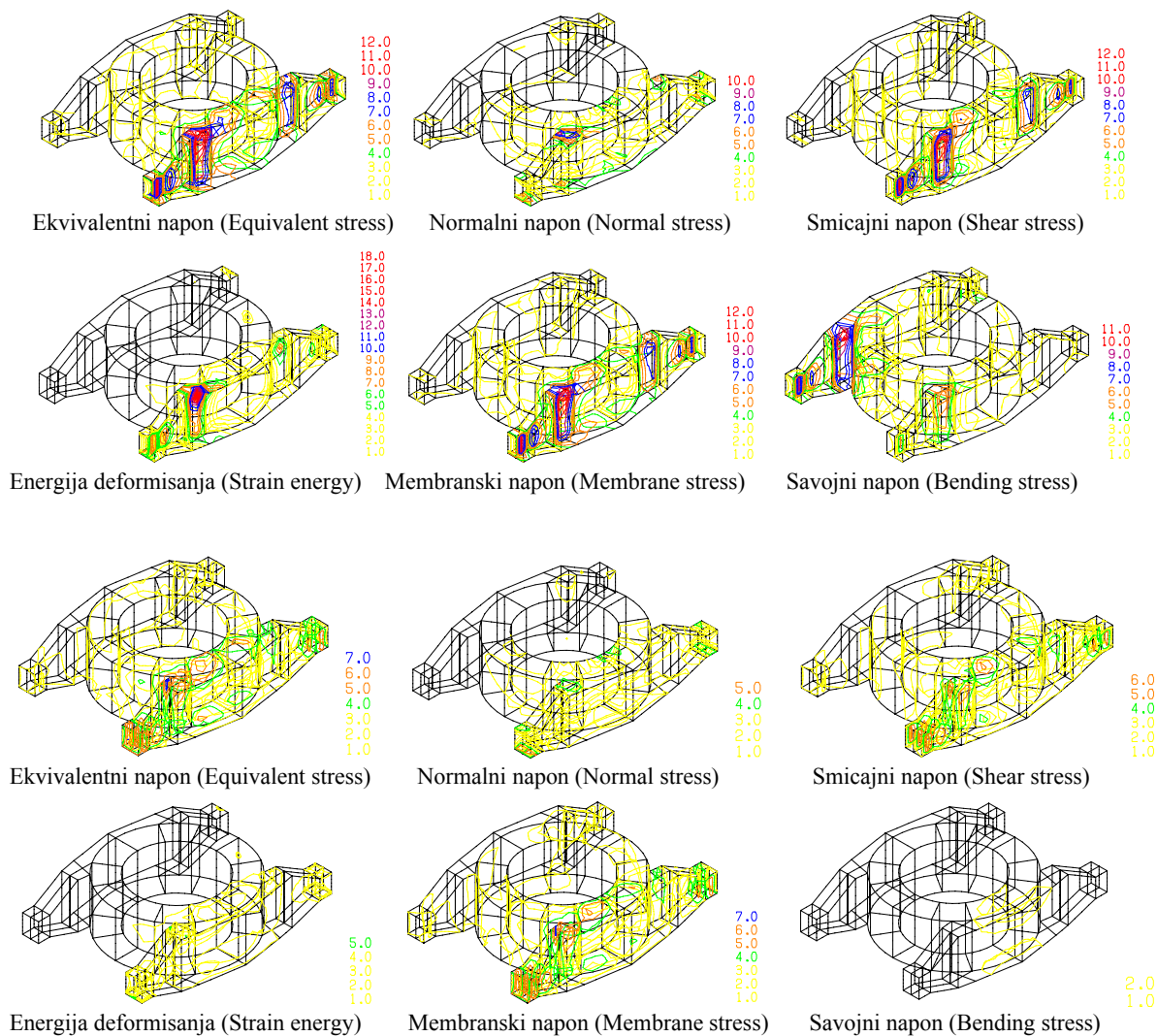
- vertical plates have the largest stress and strain energy,
- horizontal plates have a high stress level in a small area,
- the stress level in cylinders is low in a large area, along with a high percentage of the stress and energy,
- diaphragms pose the least significant effect on behaviour.

Loše ponašanje donje gradnje možemo popraviti dodavanjem vertikalnih ploča. Takođe, ponašanje bi se značajno popravilo povećanjem debljine horizontalnih ploča i cilindra, ali je ovo tehnički neopravdano.

Dodavanje vertikalnih ploča izvodi se zatvaranjem obe strane četiri nosača "I" preseka. Detaljno je ispitan uticaj debljine dodatih ploča. Usvojena debljina spoljašnjih ploča je 25 mm, a unutrašnjih 15 mm.

Inappropriate lower assembly structural behaviour can be repaired by adding vertical plates. Behaviour would also be significantly improved by increasing horizontal plate and cylinder thickness, but this is technically not reasonable.

The vertical added plates cover both sides of four "I" cross-sectional beams. The effect of added plate thickness was tested in detail. Approved plate thicknesses are 25 mm and 15 mm, for outer and inner plates, in respect.



Slika 14. Raspodela napona [kN/cm^2] i energije deformisanja [kNcm]

Figure 14. Stress [kN/cm^2] and strain energy [kNcm] distribution.



Slika 15. Rekonstrukcija donje gradnje
Figure 15. Reconstruction of lower assembly.

Uvođenje novih vertikalnih ploča dovodi do značajnog poboljšanja ponašanja donje gradnje kroz:

- smanjenje maksimalne deformacije za 33,9%,
- smanjenje maksimalnog napona za 42,3%,
- rasterećenje cilindara, horizontalnih ploča i postojećih vertikalnih ploča,
- smanjenje energije deformisanja za 24,2%.

Prikaz konstrukcije pre i posle rekonstrukcije dat je na sl. 15.

SANACIJA I REKONSTRUKCIJA GORNJE GRADNJE BAGERA 800 O&K (DRMNO KOSTOLAC)

Bager je imao stalna pucanja na gornjoj gradnji. Poslednja prslina na spoju cilindra i donje horizontalne ploče je bila dužine 2 m. Takođe, dolazilo je do pojave prslina na vrhu stuba. Iznalaženje uzroka pucanja zahteva detaljnu dijagnostiku čvrstoće gornje gradnje za sve slučajeve dinamičkog opterećenja. Prikaz računskog modela, najnepovoljnijeg opterećenja, deformisane gornje gradnje i elemenata rekonstrukcije dati su na sl. 16. Raspodela napona i energije deformisanja data je na sl. 17. Rekonstruisana gornja gradnja data je na sl. 18.

Zaključak dijagnostike je: velika deformacija, vrlo visok nivo napona i koncentracije napona, izražen normalni membranski napon i najveći naponi i energija deformisanja na istom mestu. Ovakvo ponašanje olakšava rešenje problema.

Adding new vertical plates has led to significant improvement of lower assembly structural behaviour, such as:

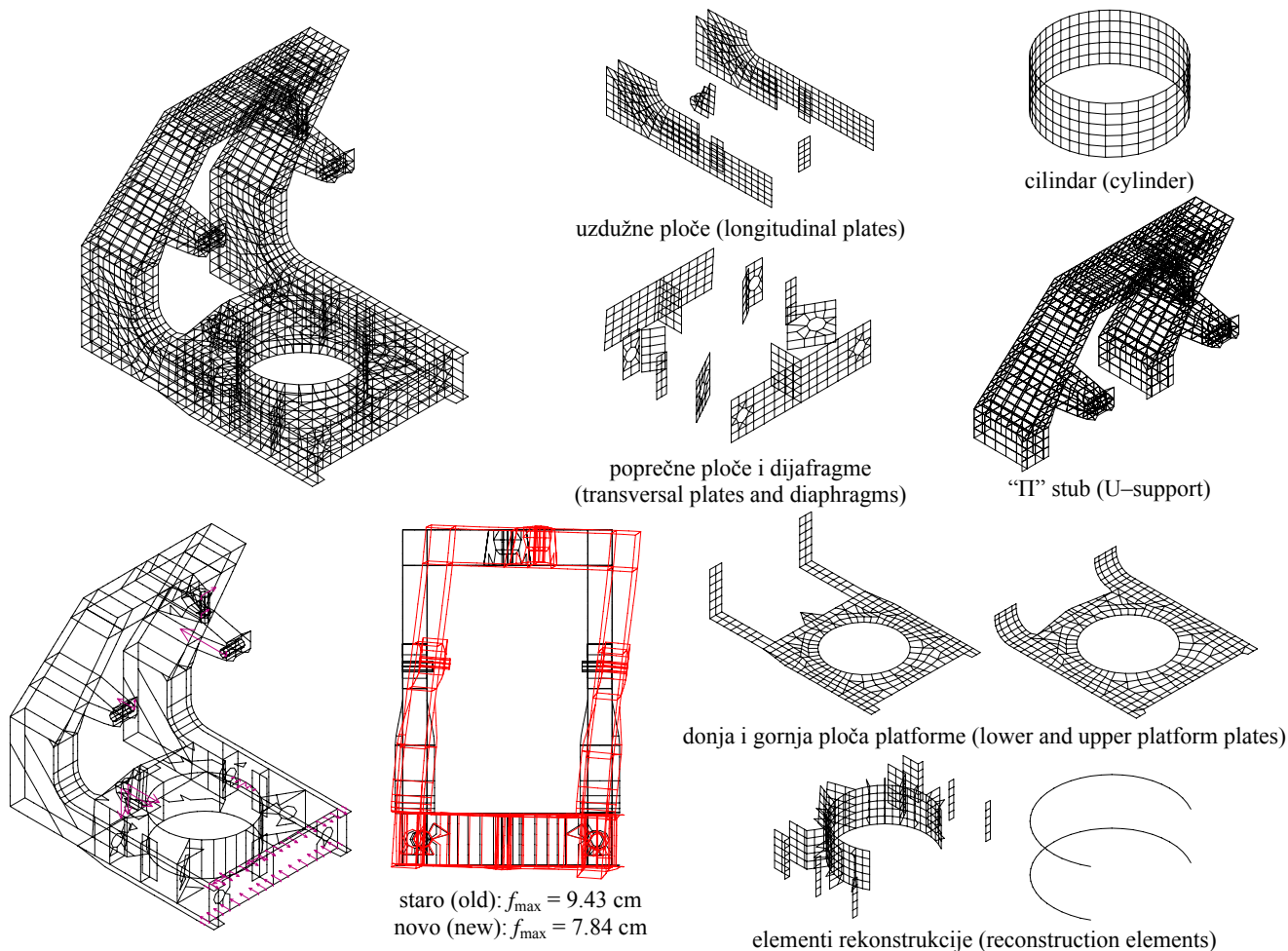
- maximum strain decrease by 33.9%,
- maximum stress decrease by 42.3%,
- stress relaxing of cylinders, horizontal plates, and existing vertical plates,
- strain energy decrease by 24.2%.

The state before and after reconstruction is shown in Fig. 15.

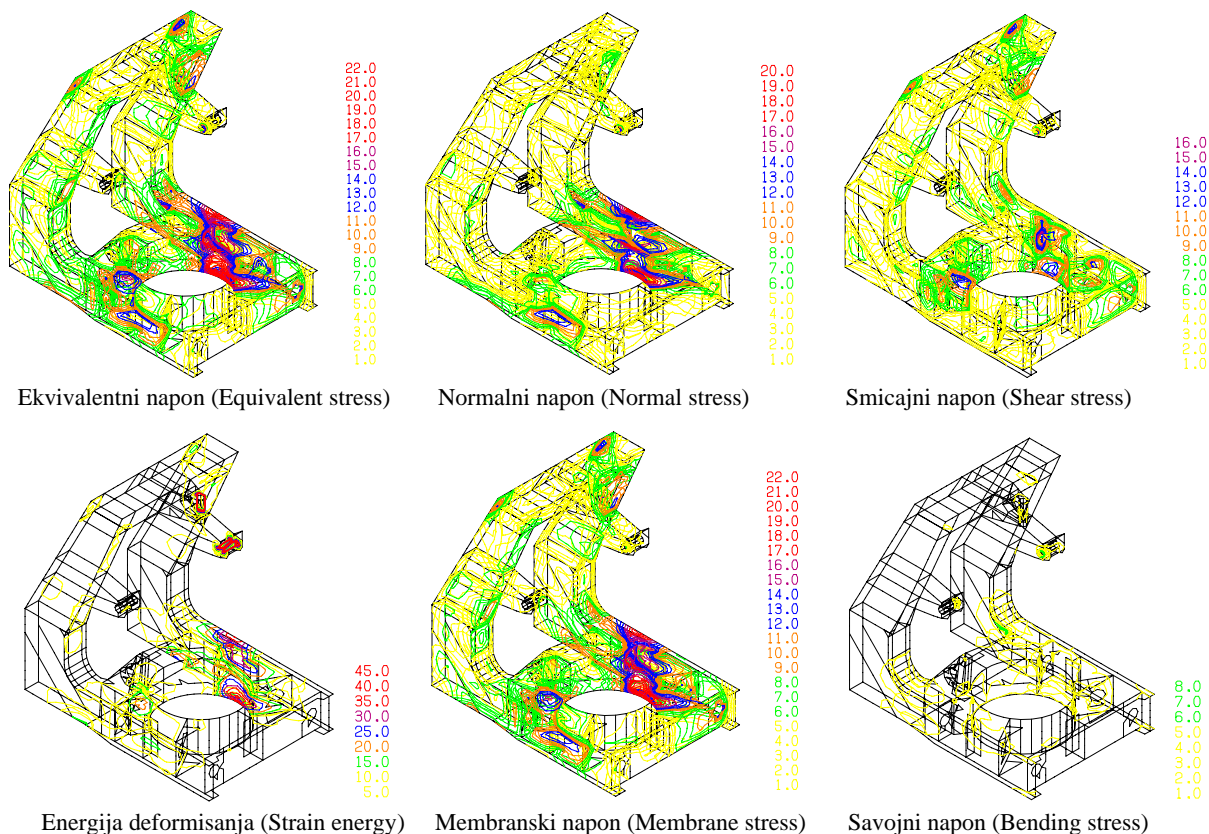
REPAIR AND RECONSTRUCTION OF EXCAVATOR LOWER ASSEMBLY, 800 O&K (DRMNO KOSTOLAC)

The excavator suffered constant cracking in the lower assembly. The hindering crack in the cylinder–lower horizontal plate joint was 2 m long. Also, cracks appeared at the top of support. Determining causes for cracking requires detailed structural strength diagnostics of the upper assembly for all dynamic loading cases. The computational model, worst load case, deformed structure pattern and reconstructed elements are shown in Fig. 16. Stress and strain energy distributions are given in Fig. 17. The reconstructed upper assembly is shown in Fig. 18.

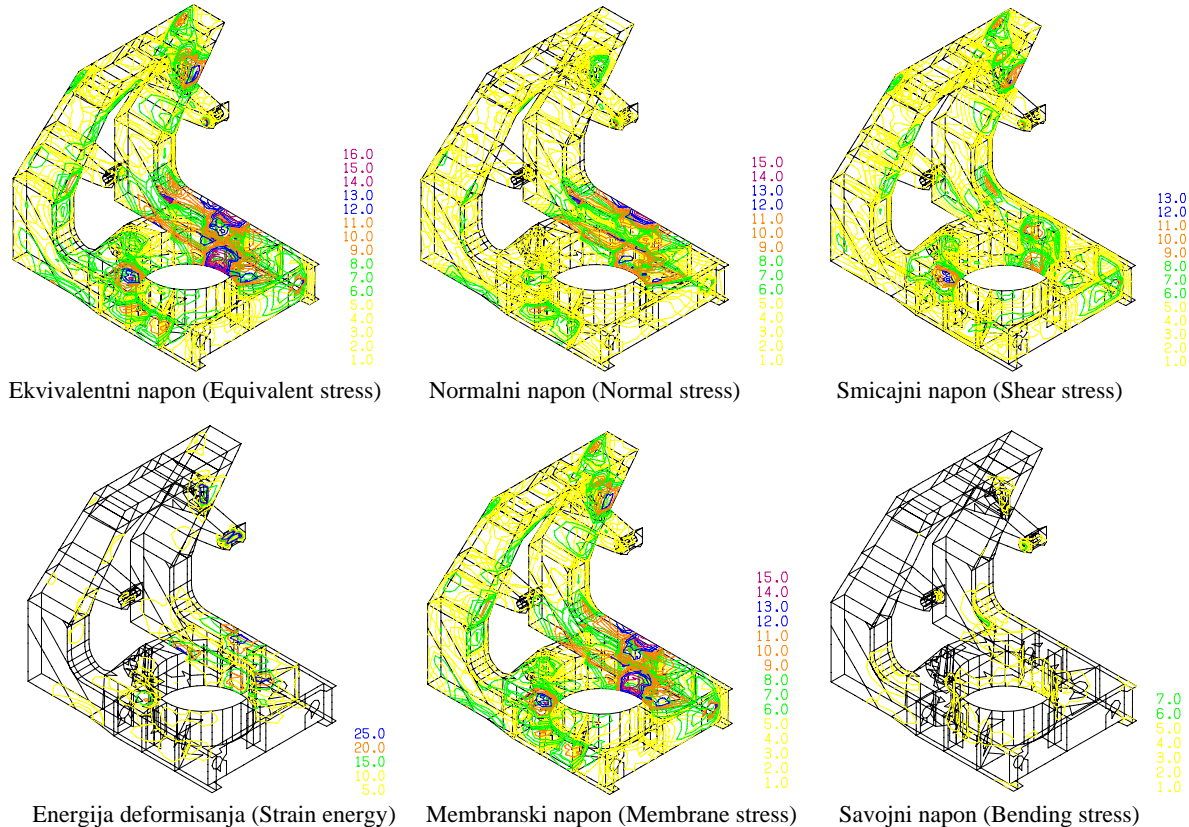
Diagnostics conclude the following: large strain, very high level of stress and its concentration, high normal membrane stress and strain energy appearing in the same location. Such behaviour makes the problem easier to solve.



Slika 16. Model gornje gradnje bagera, njegova deformacija i elementi rekonstrukcije
Figure 16. The upper assembly structural model, its strain and reconstruction elements.



Slika 17. Raspodela napona [kN/cm²] i energije deformisanja [kNcm] stare konstrukcije
 Figure 17. Stress [kN/cm²] and strain energy [kNcm] distribution of the old construction.



Slika 18. Raspodela napona [kN/cm²] i energije deformisanja [kNcm] rekonstruisane gornje gradnje
 Figure 18. Stress [kN/cm²] and strain energy [kNcm] distributions of the reconstructed upper assembly.

Prikaz raspodela parametara dijagnostike ponašanja konstrukcije je dat u tab. 3. Vidimo da smo rasteretili donju ploču, gornju ploču i cilindar, a opteretili uzdužne ploče, što nam je bio cilj.

Ovom modelu je dodata i donja gradnja sa ciljem da potvrdimo ponašanje i tačno odredimo opterećenje između donje i gornje gradnje na mestu njihove veze (ležaj). Očrkivano ponašanje je potvrđeno (sl. 19).

Structural behaviour of diagnostic parameter distribution is given in Table 3. Apparently, both lower and upper plates are relaxed, as well as the cylinder, while longitudinal plates are loaded, which was the goal.

The lower assembly is added to this model in order to confirm the behaviour and accurately determine the load in between the lower and upper structures at the connection (bearing). Expected behaviour is confirmed (Fig. 19).

Tabela 3. Raspodela parametara dijagnostike ponašanja konstrukcije—Table 3. Distribution of parameters for diagnostic structural behaviour.

	σ_{max} [kN/cm ²]		mem./sav mem/bend [%]		σ/τ [%]		E_d [%, kNcm]	
	Staro (Old)	Novo (New)	Staro (Old)	Novo (New)	Staro (Old)	Novo (New)	Staro (Old)	Novo (New)
Uzdužna ploča (Longit. plate)	17	13	15.6/2.8	15.2/2.6	12.4/6	12/5.8	16.3	17.9
Poprečna ploča (Transv. plate)	17	11	7.7/1	8.9/1.2	4.5/4.3	5.4/4.6	4.6	4.2
Cilindar (Cylinder)	22	13	7/2.3	5/1.9	5.6/3.5	4.4/2	4.8	4.2
Donja ploča (Lower plate)	22	16	14.9/1.5	13.7/1.3	13/3.5	11.5/3	19.2	17
Gornja ploča (Upper plate)	20	14	12.9/2.4	12.7/2	12.2/3.1	11.5/3.2	17.5	17.6
Stub (Support)	14	13	27.8/3.9	28.3/4.3	20.5/11.4	21.2/11.3	29.3	28.1
Grede (Beams)				2.4/0.4		3/0.1	8.3	11
Suma (Total)			86.1/13.9	86.3/13.7	68.2/31.8	69 / 31	13500	11200



Slika 19. Model, rekonstrukcija i ekvivalentni napon donje i gornje gradnje
Figure 19. The model, reconstruction and equivalent stress of the lower and upper assembly.

OTKLANJANJE UZROKA POPUŠTANJA ULAZNIH LEŽAJA REDUKTORA KOPANJA BAGERA SRS2000 MANTAKRAF (*DRMNO KOSTOLAC*)

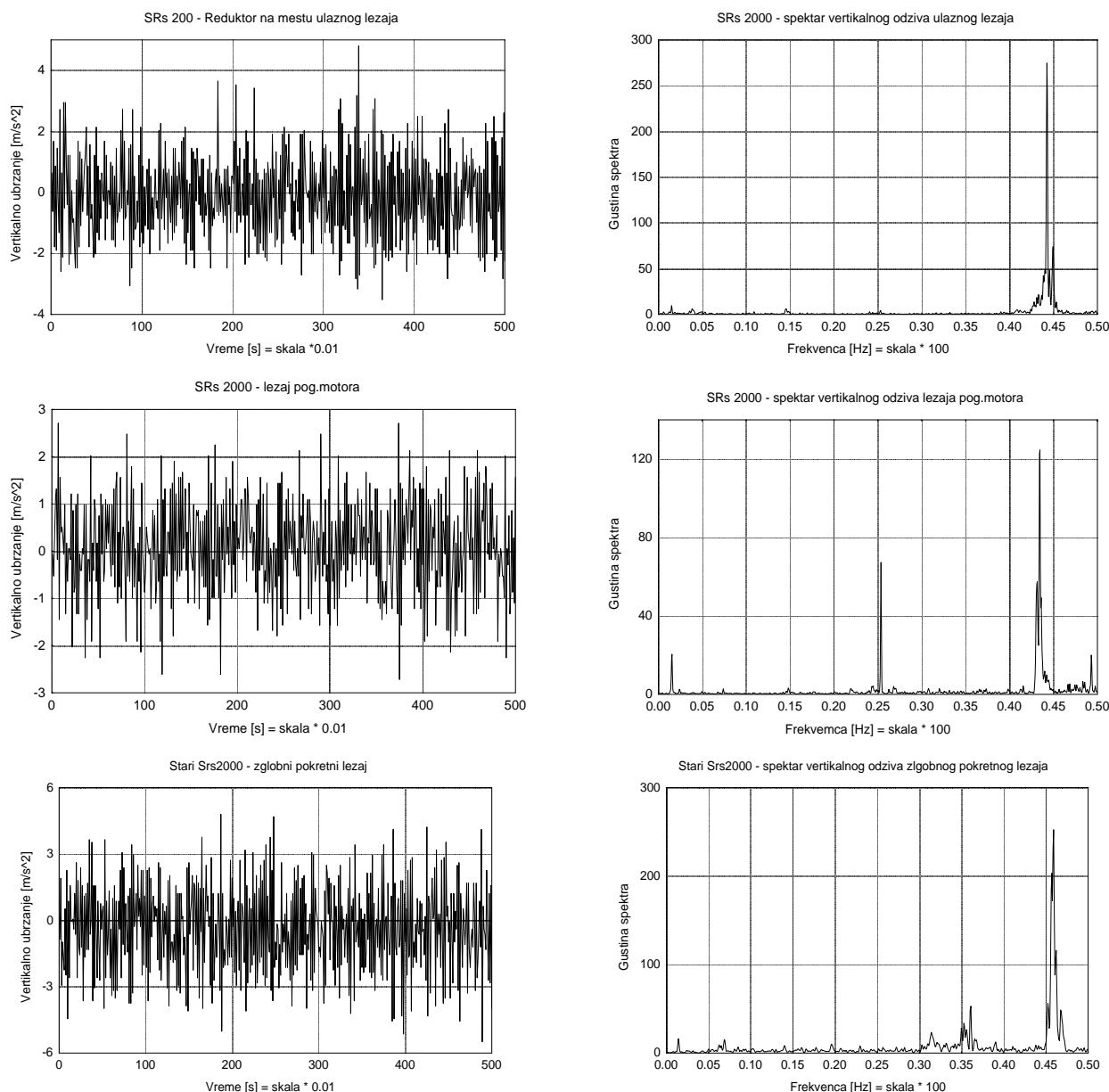
Izvedena kombinovana numeričko-eksperimentalna dijagnostika dinamičkog ponašanja pogona daje kvalitetne parametre uzroka učestalog popuštanja ležaja ulaznih vratila reduktora (posle 7 dana rada). Rad pogona bagera je praćen u tri navrata i pri tom su merena ubrzanja ležaja reduktora i motora kao i noseće konstrukcije u sva tri pravca. Vizuelnim pregledom ustanovljeno je da je veza noseće konstrukcije pogonskih motora i reduktora bila olabavljena, kao i da postoji veći zazor u osovine sfernog oslonca reduktora. Na sl. 20. prikazana su izmerena ubrzanja pogona u vremenskom i frekventnom domenu. Vidimo da su ubrzanja na granici dozvoljenog, a da je oscilovanje oba ležaja, na oko 44 Hz, jako nepovoljno. Radni broj obrtaja motora izaziva pobudnu frekvenciju 24.6 Hz (14800/min) i narednu $2 \times 24.6 = 49.2$ Hz. Prisustvo oscilovanja ležaja motora na oko 1.5 Hz, koja je bliska frekvenciji kopanja govori nam da se noseća struktura konzolno postavljenih poprečnih

RESOLVING DETERIORATION CAUSES ON DRIVING TRANSMISSION BEARINGS OF EXCAVATOR SRS2000 MANTAKRAF (*DRMNO KOSTOLAC*)

Combined numerical-experimental diagnostics of dynamic power system behaviour gives qualitative parameters for the cause of frequent bearing damage at the transmission driving shaft (after 7 days service). The excavator power system was monitored three times, during which the acceleration of motor- and transmission bearings, as well as the support structure were measured in all three directions. Visual control showed that the supporting structure and the power system/transmission joint had loosened, with significant gap in the spherical support transmission axle. Figure 20 shows measured acceleration in time and frequency domain. Accelerations are close to allowed, and oscillations of both bearings of about 44 Hz, are unacceptable. The cycles of the motor had caused an induced frequency of 24.6 Hz (14800/min) and next frequency of $2 \times 24.6 = 49.2$ Hz. Oscillations of motor bearings, about 1.5 Hz, being close to digging frequency suggests that the support structure of

motora mora pojačati. Bliskost druge pobudne frekvencije motora i frekvencije ležaja reduktora govori da reduktor, ili ulazno vratilo, ima lošu dinamičku karakteristiku (mora imati prvu sopstvenu frekvenciju veću od 50 Hz). Smanjenje frekvencije izazvano je ugradnjom teže spojnice i pomeranjem njenog težišta od ulaznog ležaja za oko 150 mm. Takođe, ovde je prikazano oscilovanje pokretnog zglobnog oslonca na kome vidimo jako izraženo oscilovanje ovog ležaja sa velikim ubrzanjima i amplitudom odziva.

cantilever-placed transversal motors must be reinforced. The similarity between induced frequencies of the motor and transmission bearings suggests that either the transmission or the driving shaft have very poor dynamic characteristics (the first eigen-frequency should be above 50 Hz). The frequency drop is caused by installed heavy couplings and from the dislocating their centre of mass to 150 mm from driving bearings. Free joint support oscillations with highly developed oscillations in bearings and with high accelerations and response amplitudes are also shown.



Slika 20. Vertikalno ubrzanje u vremenskom (levo) i gustina spektra u frekventnom domenu (desno)
Figure 20. Vertical acceleration in time (left) and spectrum density in frequency domain (right).

Računski dinamički model ulaznog vratila i prvi oblik oscilovanja sa uticajem težine spojnice na sopstvenu frekvenciju su dati na sl. 21. Težina dela spojnice vrlo nepovoljno utiče na prvu sopstvenu frekvenciju (mora biti lakša od 400 kg). Redukovani računski dinamički model celog

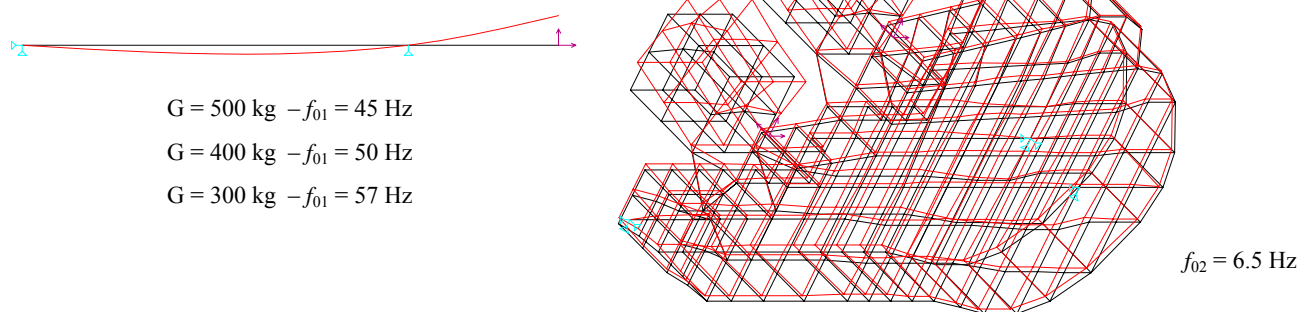
The numerical model of the driving shaft and first form oscillations with coupling weight affecting its eigen-frequency value is shown in Fig. 21. The coupling weight has a very negative effect on first eigen-frequency (the coupling must be lighter than 400 kg). A reduced numerical dynami-

reduktora sa motorima, kao i drugi oblik oscilovanja, prikazani su na sl. 21. Model potvrđuje nepovoljan uticaj vertikalnog oscilovanja motora koje se javlja i na dosta drugih frekvencija.

Uspešan rad reduktora u naredna četiri meseca (do zamenе reduktora iz drugih razloga) obezbeđen je samo povećanjem krutosti nosača poprečnih motora. Zamena teže spojnice lakšom nija bila moguća.

cal model of the whole transmission with motors, as well as the second form of oscillations are shown in Fig. 21. This model confirms negative effects of the motor's vertical oscillation that occur at many other frequency values.

Successful transmission operation in the following four months (until replacement for other reasons) was achieved only by increasing the rigidity of transversal motor beams. It was impossible to replace the coupling with a lighter one.



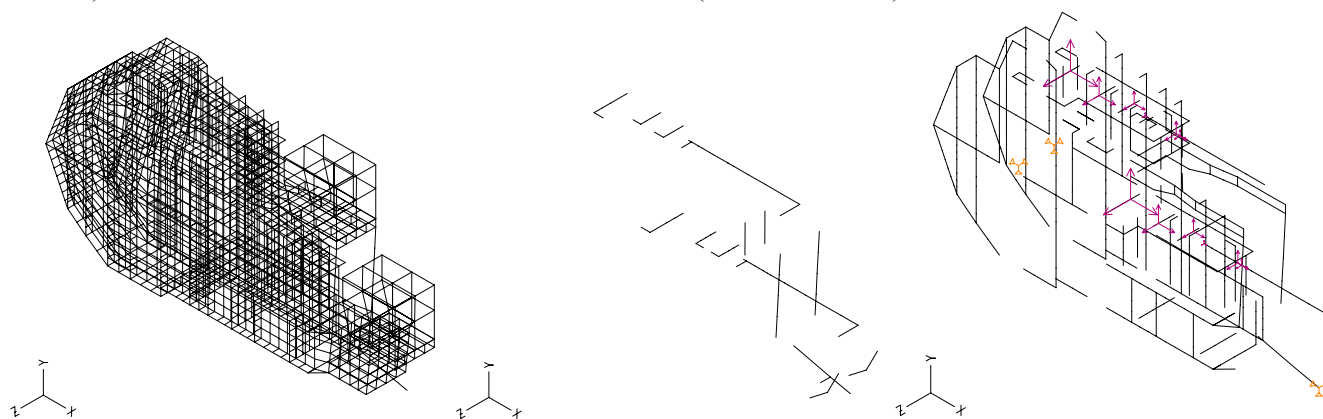
Slika 21. Dinamički model ulaznog vratila i reduktora sa motorima
Figure 21. Dynamic model of the driving shaft and transmission with motors.

DIJAGNOSTIKA DINAMIČKE ČVRSTOĆE POGONA KOPANJA BAGERA SRS2000 (DRMNO KOSTOLAC)

Račinski model reduktora sa nosačem, vratilima i pogonskim motorima prikazan je na sl. 22. U tabeli 4 dato je prvih osam sopstvenih frekvencija za različite načine postavljanja spojnice i njene težine. Broj obrta pogonskog elektromotora iznosi 980 min^{-1} , što izaziva pobudu na frekvenciji 16.3 Hz i na svim narednim umnošcima ($2 \times 16.3 = 32.6 \text{ Hz}$).

FATIGUE LIMIT DIAGNOSTICS ON EXCAVATOR POWER UNIT SRS2000 (DRMNO, KOSTOLAC)

The computational transmission model with beams, shafts and power machines is shown in Fig. 22. The first eight eigen-frequencies for variants of coupling placement and weight are given in Table 4. The number of revolutions of the electric motor is 980 min^{-1} , which creates induction at 16.3 Hz frequency, and at multiple subsequent values ($2 \times 16.3 = 32.6 \text{ Hz}$).



Slika 22. Računski model reduktora
Figure 22. Computational model of the transmission.

Tabela 4. Prvih osam sopstvenih frekvencija [Hz] za različite načine postavljanja spojnice i njene težine
Table 4. The first eight eigen-frequencies [Hz] for variants of coupling placement and weight.

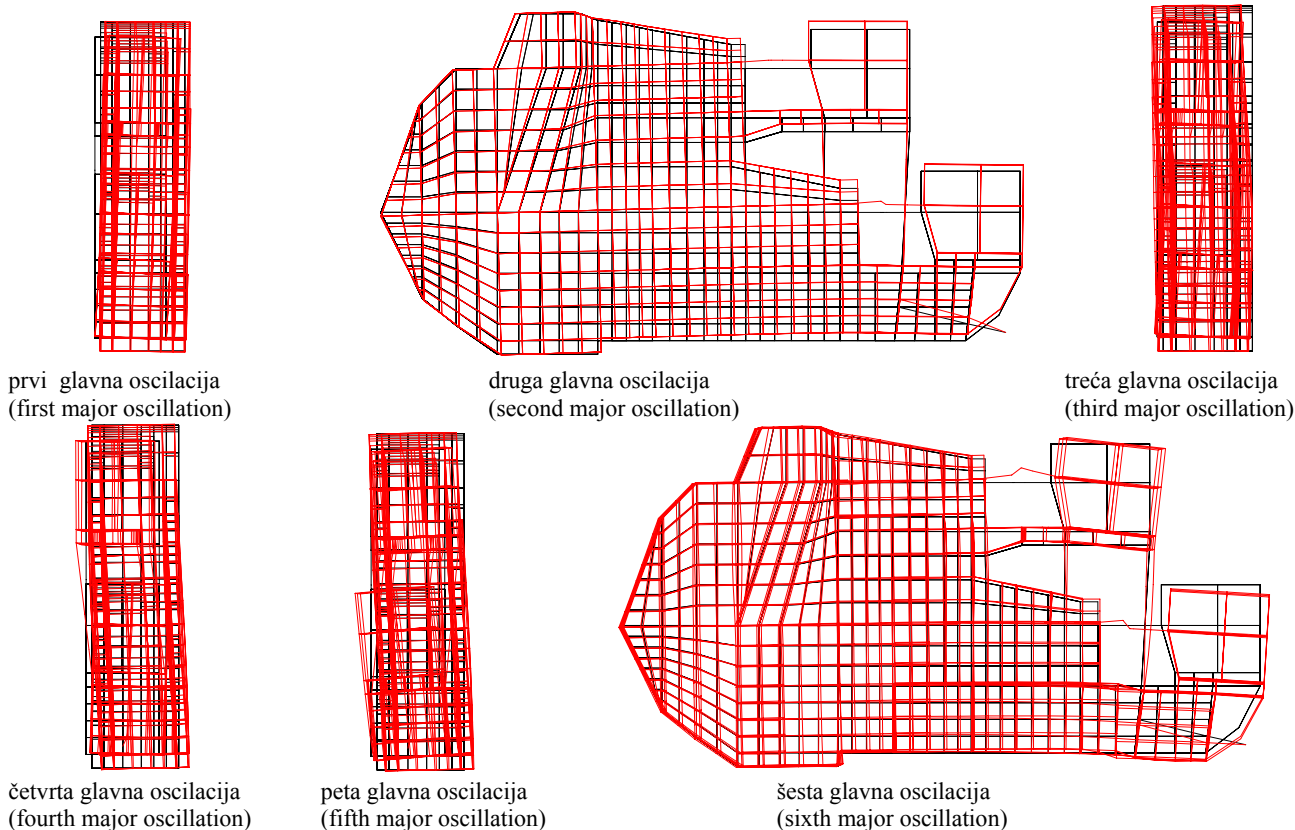
teži deo spojnice (coupling heavier side)	f_{01}	f_{02}	f_{03}	f_{04}	f_{05}	f_{06}	f_{07}	f_{08}
300 kg mase na reduktoru (mass on transmission)	8.4	14.6	18.8	21	22.2	32.2	34	35.2
400 kg mase na reduktoru (mass on transmission)	8.7	14.5	18.7	20.9	22.2	30	31.8	32.1
300 kg mase na pog. motoru (mass on motor)	8.7	14.7	18.8	20.9	22.1	34.5	36.8	42.5
400 kg mase na pog. motoru (mass on motor)	8.6	14.6	18.7	20.8	22.1	34.3	36.5	42.5

Odluka o postavljanju težeg dela spojnice na strani reduktora ili motora se mora doneti posle numeričko-eksperimentalne dijagnostike.

Prvih šest oblika oscilovanja reduktora prikazani su na sl. 23.

Placing the heavier coupling side on the transmission or on the motor must be decided after numerical-experimental diagnosis.

The first six forms of transmission oscillations are presented in Fig. 23.



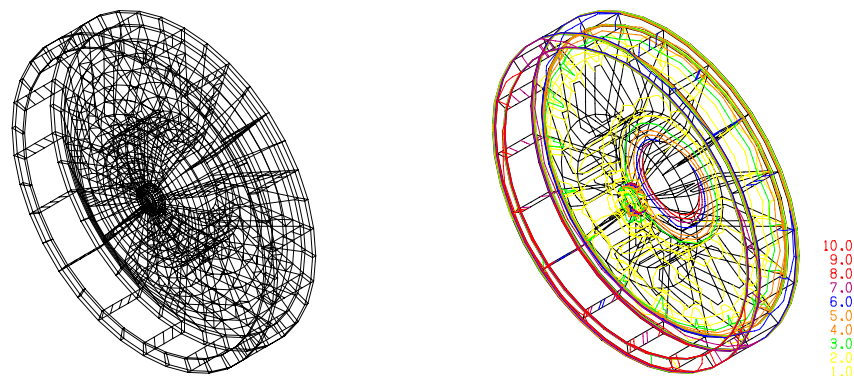
Slika 23. Prvih šest oblika oscilovanja reduktora
Figure 23. The first six forms of transmission oscillations.

DEFINISANJE ELEMENATA REVITALIZACIJE POGONSKOG SISTEMA BAGERA SRS1300 MANTAKRAF (DRMNO, KOSTOLAC)

Dijagnostika statičkog ponašanja radnog točka SchRs1300. Računski model radnog točka i ekvivalentni napon prikazani su na sl. 24. Opterećenje predstavlja celokupni moment kopanja prenet samo na jednu koficu. Ponašanje samog radnog točka je izuzetno povoljno. Detaljnija analiza ponašanja nije neophodna.

DEFINING REVITALISING ELEMENTS FOR EXCAVATOR POWER UNIT SRS1300 MANTAKRAF (DRMNO, KOSTOLAC)

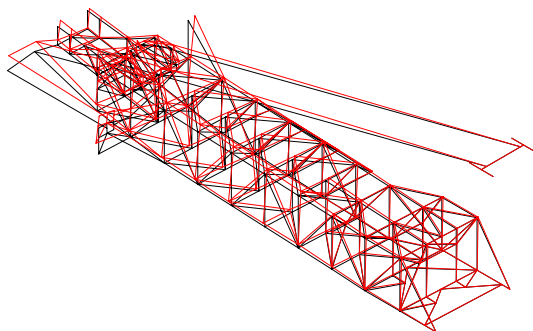
The static diagnostic behaviour of operating wheel SchRs1300. The operating wheel computational model and equivalent stress are shown in Fig. 24. The load represents the entire digging moment reduced to only one bucket. The operating wheel behaviour is very positive. There is no need for more detailed analysis of behaviour.



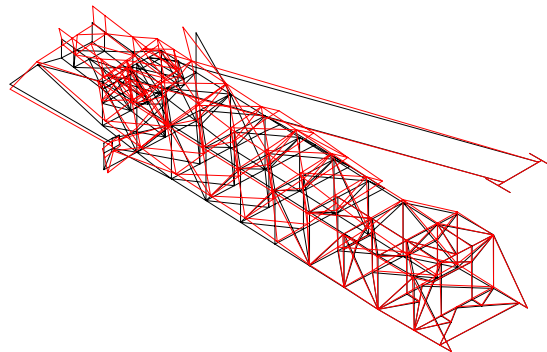
Slika 24. Računski model i ekvivalentni napon [kN/cm²] radnog točka sistema za kopanje
Figure 24. Computational model of digging system operating wheel and equivalent stress [kN/cm²].

Dijagnostika dinamičkog ponašanja strele radnog točka SchRs1300. Sledi prikaz proračunatih glavnih oblika oscilovanja strele radnog točka za dva krajnja položaja strele (položaji A i B).

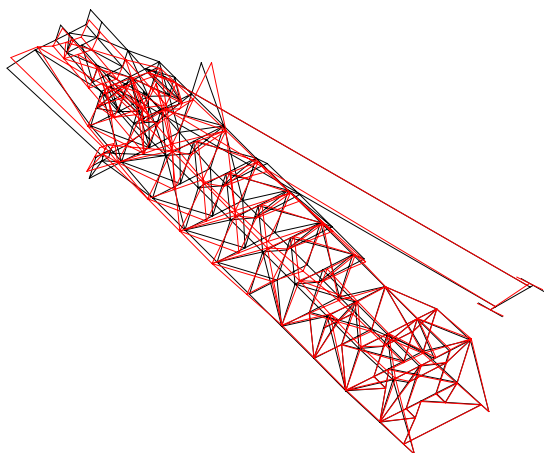
Dynamic behaviour diagnostics of the operating wheel cantilever beam SchRs1300. Shown below are major oscillation forms of the operating wheel for two outermost cantilever positions (A and B).



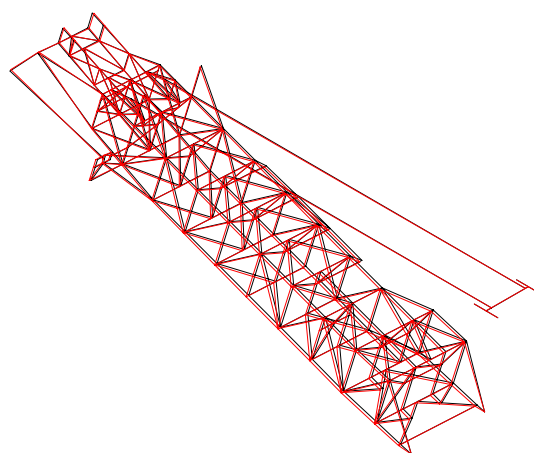
Položaj (Position) A: $f_{01} = 0.8 \text{ Hz}, f_{02} = 1.3 \text{ Hz}$



Položaj (Position) A: $f_{03} = 2.3 \text{ Hz}, f_{04} = 3.3 \text{ Hz}$



Položaj (Position) B: $f_{01} = 0.8 \text{ Hz}, f_{02} = 1.6 \text{ Hz}$



Položaj (Position) B: $f_{03} = 2.7 \text{ Hz}, f_{04} = 3.4 \text{ Hz}$

Slika 25. Glavni oblici oscilovanja strele radnog točka položaje A i B

Figure 25. Major oscillating forms of operating wheel cantilever in positions A and B.

Glavni element ove dijagnostike predstavlja definisanje opsega broja istresaja (broj vedrica \times broj obrta radnog točka). Broj istresaja ne sme biti u korelaciji sa sopstvenim oscilacijama strele radnog točka. Broj istresaja na radnom točku sa stanovišta dinamike strele treba da se kreće u intervalu $(1.6 \div 2.3 \text{ Hz}) \times 60 \text{ sec} = 96 \div 138$, odnosno za točak sa 23 kofice broj obrta je između 4.17 i 6 min^{-1} .

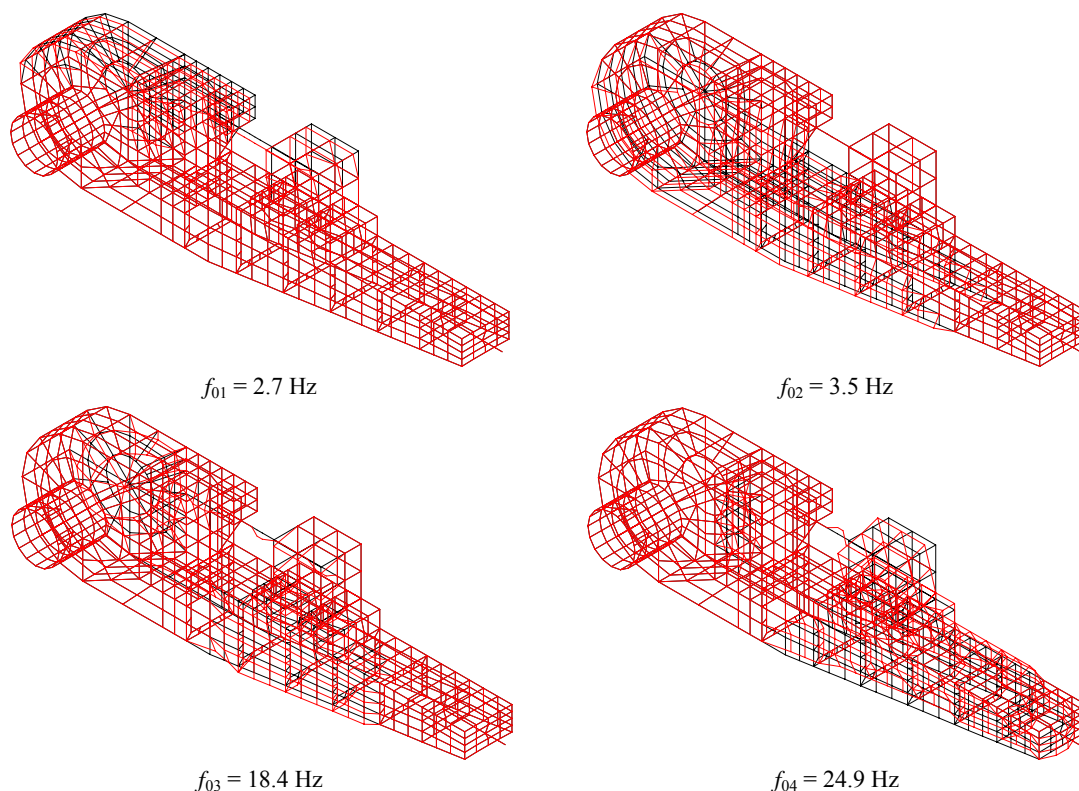
Dijagnostika dinamičkog ponašanja reduktora kopanja bagera SchRs1300. Broj obrta elektromotora je 1480 min^{-1} , pa time imamo prvu i drugu prinudnu pobudnu frekvenciju $1480/60 = 24.66 \text{ Hz}$, $1480/60 \times 2 = 49.32$. Prinudna pobudna frekvencija kopanja je broj istresaja u sekundi, odnosno, u ovom slučaju 2.65 Hz . Kako prva sopstvena frekvencija ulaznog vratila iznosi 54 Hz , isto ima dobro ponašanje. Dinamički modeli reduktora kopanja dati su na sledećoj sl. 26.

Osnovni nedostaci reduktora su: veoma dugačka momentna poluga; nedovoljno krut sklop ulaznog vratila reduktora, vratila elektromotora i samog elektromotora i velike težine, koja nepovoljno utiče na raspodelu opterećenja zatega i stuba bagera (moment uvijanja strele je velik u odnosu na podužnu osu).

The main diagnostic element is defined by the unloading range (number of buckets \times operating wheel revolutions). The unloading number must correlate to eigen-value oscillations of the operating wheel cantilever beam. From the cantilever dynamics point of view, the number of unloads should be within $(1.6 \div 2.3 \text{ Hz}) \times 60 \text{ sec} = 96 \div 138$, i.e. for a 23 bucket wheel, the revolutions should be 4.17 to 6 min^{-1} .

Dynamic behaviour diagnostics of the excavator digging transmission SchRs1300. The number of cycles of the electric-motor is 1480 min^{-1} , so the first and second forced induced frequency, in respect, are $1480/60 = 24.66 \text{ Hz}$, and $1480/60 \times 2 = 49.32$. The forced induced digging frequency in this case equals 2.65 Hz . Since the first eigen-frequency of the driving shaft is 54 Hz , it also shows good behaviour. Dynamic models for the digging transmission are shown in Fig. 26.

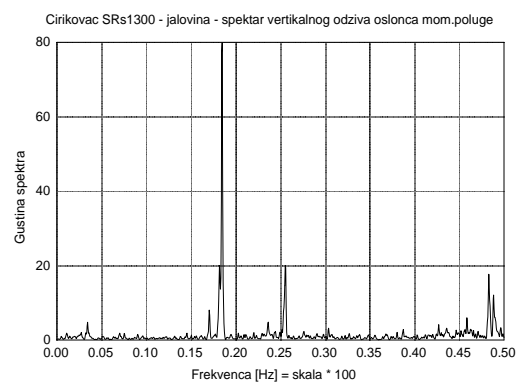
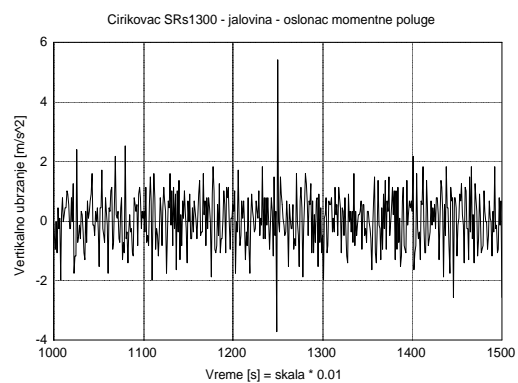
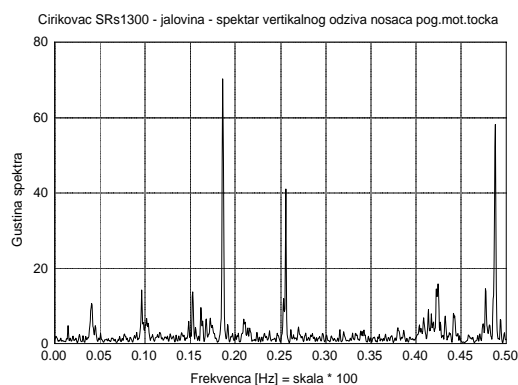
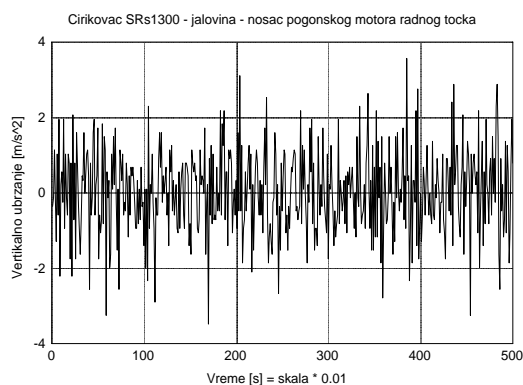
The general shortcomings of transmission are: very long moment lever; insufficiently rigid assembly of the driving transmission shaft, the electric-motor shaft, and the electric motor itself; and large weight that negatively affects the distribution of load on ties and support (the torsion moment of the cantilever has a large longitudinal axis component).



Slika 26. Prva četiri sopstvene frekvencije modela
Figure 26. First four eigen-frequencies of the model.

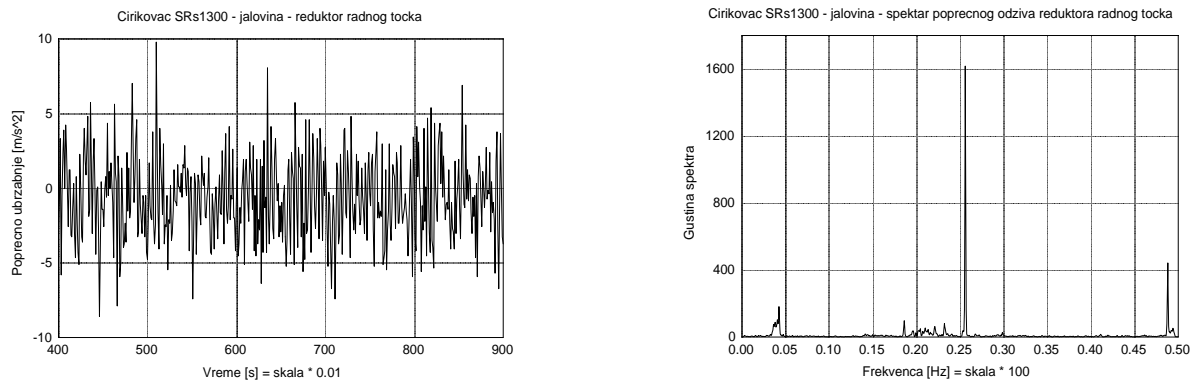
Ekspperimentalno merenje. Proračun je verifikovan izvedenim merenjem ubrzanja na sistemu za kopanje u radu ovog bagera. Merenje je izvedeno više puta. Sledi prikaz rezultata merenja ubrzanja u vremenskom i frekventnom domenu (sl. 27).

Experimental measurements. The calculation was verified by measurements on a digging system during excavator operation. Measurements were taken several times. Some acceleration measurements in real-time and frequency domain are shown below (Fig. 27).



(nastavak na sledećoj strani)

(continued on next page)



Slika 27. Poprečno ubrzanje u vremenskom (levo) i gustina spektra u frekventnom domenu (desno)
Figure 27. Transversal acceleration in time (left) and spectrum density in frequency domain (right).

Komentar merenja: ubrzanja uveliko prelaze dozvoljenu vrednost ($a_{dmax} = 2 \text{ m/s}^2$); odziv konstrukcije sistema za kopanje ima jak signal na frekvencijama 3, 4, 12, 14, 18, 25 i 49 Hz i nešto slabiji signal na frekvencijama 2, 5, 7, 9, 13, 15 i 23 Hz, koje su u uskoj korelaciji sa pobudama i sopstvenim frekvencijama reduktora kopanja, odnosno, reduktor kopanja može veoma lako ući u rezonantno područje rada. Na ovom kopu reduktor je doživeo havariju. Ovaj tip reduktora imao je havarije i još uvek ima probleme u radu i na drugim kopovima, što potvrđuje identifikovano loše ponašanje reduktora. Predlaže se zamena reduktora kopanja, odnosno, njegova globalna revitalizacija.

DIJAGNOSTIKA ČVRSTOĆE VEDRICA I OPTIMIZACIJA

Sledi prikaz dijagnostike čvrstoće više vedrica.

Komentar vedrice bagera SRs630 O&K, kop Tamnava zapadnog polja: deformacija zadovoljavajuća uz visok napon i koncentraciju; dominantno prisustvo smicajnog i savojnog napona, što nije dobro; uvođenjem 4 oslonca kod ove vedrice pogoršavamo ponašanje.

Komentar vedrice bagera SchRs800 O&K, kopa Drmno Kostolac: izuzetno visok nivo deformacije i napona kao i njegove koncentracije; dominantno prisustvo smicajnog i savojnog napona, što nije dobro; uvođenje 4 oslonca kod ove vedrice je poboljšalo ponašanje.

Komentar vedrice bagera SRs630 O&K, kop polje D: izuzetno velika deformacija, napon i koncentracija; zadnji deo vedrice, zbog velike deformacije i zazora između nje i lanca, dolaze u kontakt nakon neke vrednosti opterećenja, pa time rezultati nisu precizni; veoma izraženo prisustvo smicajnog i savojnog napona, što nije dobro.

Komentar o razvojnom projektu jedne vedrice: deformacija zadovoljavajuća; napon i koncentracija visoki.

Komentar optimalne varijante br. 1: veoma nizak nivo deformacije i napona uz minimalno prisustvo koncentracije napona; težina izuzetno mala; energija deformisanja najmanja; raspodela napona povoljna.

Komentar optimalne varijante br. 2: nizak nivo deformacije i napona uz malo prisustvo koncentracije napona; težina je na nivou postojećih; energija deformisanja zadovoljavajuća; raspodela napona nešto nepovoljnija.

Comment on measuring: the accelerations overpasses allowed values ($a_{dmax} = 2 \text{ m/s}^2$); the response of the digging system is a strong signal at frequencies 3, 4, 12, 14, 18, 25, and 49 Hz, and slightly weaker at frequencies 2, 5, 7, 9, 13, 15, and 23 Hz, and these frequencies are tightly correlated to the induced and eigen frequencies of digging transmission, i.e. the transmission may easily approach resonance in operation. This transmission had suffered failure. This type of transmission had failures and still has operating problems also at other basins. This confirms that poor behaviour is identified. Replacement, or global revitalisation of the digging transmission is recommended.

BUCKET STRENGTH DIAGNOSTICS AND OPTIMISATION

Strength diagnostics for several buckets are shown below.

Comment on excavator buckets SRs630 O&K, basin Tamnava zapadno polje: satisfying strains with high stress and stress concentration levels; dominant presence of shear and bending stresses, which is not convenient; addition of 4 supports to this bucket had worsened its behaviour.

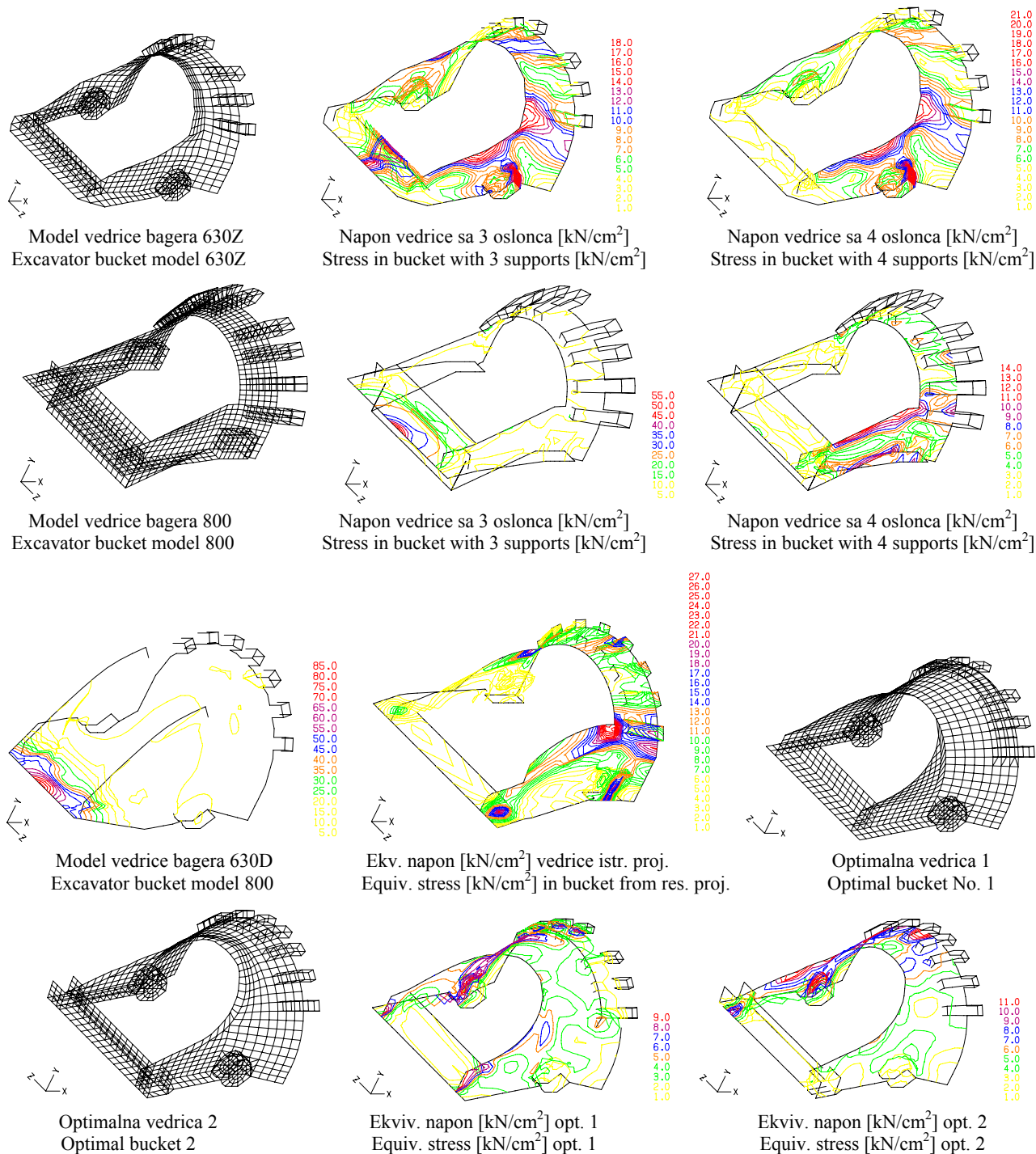
Comment on excavator buckets SchRs800 O&K, basin Drmno Kostolac: very high strain and stress levels as well as stress concentration; dominant presence of shear and bending stresses, which is inconvenient; introducing 4 supports improved the structural behaviour of this bucket.

Comment on excavator buckets SRs630 O&K, basin field D: extreme strains, stresses, and stress concentration level; rear part of the bucket will, due to large strain and gap between bucket and chain, come into contact when a certain load is reached, thus results are incorrect; very large shearing and bending stresses, which is bad.

Comment on a development project of one bucket: satisfying strain; high stress and stress concentration level.

Comment on optimal variant No. 1: very low strain and stress levels with small stress concentration; very low weight; strain energy is the lowest; stress distribution is satisfactory.

Comment on optimal variant No. 2: low strain and stress levels with minimal stress concentration; the weight is on the existing level; satisfying strain energy; stress distribution is a little less satisfying.



Slika 28. Dijagnostika čvrstoće nekoliko varijanti vedrica
Figure 28. Strength diagnostics for several bucket variants.

Tabela 5. Analiza ponašanja vedrica. Table 5. Analysis of bucket structural behaviour.

		Težina (Weight) [kg]	f_{max} [cm]	σ_{max}^{ekv} [kN/cm ²]	Mem./Sav. (Mem/Bend.) [%]	σ/τ [%]	Deform. energ. [kNcm]
SRs630 O&K TZP	3 oslonca (supp.)	600	0.47	18	41.6/58.4	50.6/49.4	88.5
	4 oslonca (supp.)		0.37	21	39/61	51.3/48.7	68.4
SchRs800 O&K Drmno	3 oslonca (supp.)	560	1.16	55	33.9/66.1	46.5/53.6	135
	4 oslonca (supp.)		0.21	13	57.8/42.2	55.5/44.5	37
SRs630 O&K		610	1.59	85	28.3/71.7	51.2/48.8	234
Novi projekt (New project)		520	0.4	27	44.4/55.6	56/44	97
Optimal ver. 1		400	0.14	9	52/47	58.5/41.5	29
Optimal ver. 2		600	0.24	11	43/57	56/44	36

Uspešna eksploatacija kofice zahteva sledeće parametre: nizak nivo deformacije (oscilovanje zuba u rezu je minimalno); nizak nivo napona i njegove koncentracije; dominantno prisustvo normalnog i membranskog napona; nizak nivo energije deformisanja vedrice.

Prikazani pristup dijagnostike definiše potrebne parametre koje jedna vedrica treba da ispuni. Takođe, on definiše potrebnu rekonstrukciju, odnosno, revitalizaciju vedrice.

DIJAGNOSTIKA STATIČKOG I DINAMIČKOG PONAŠANJA SISTEMA ZA KOPANJE BAGERA SRS1300 KOSTOLAC-DRMNO

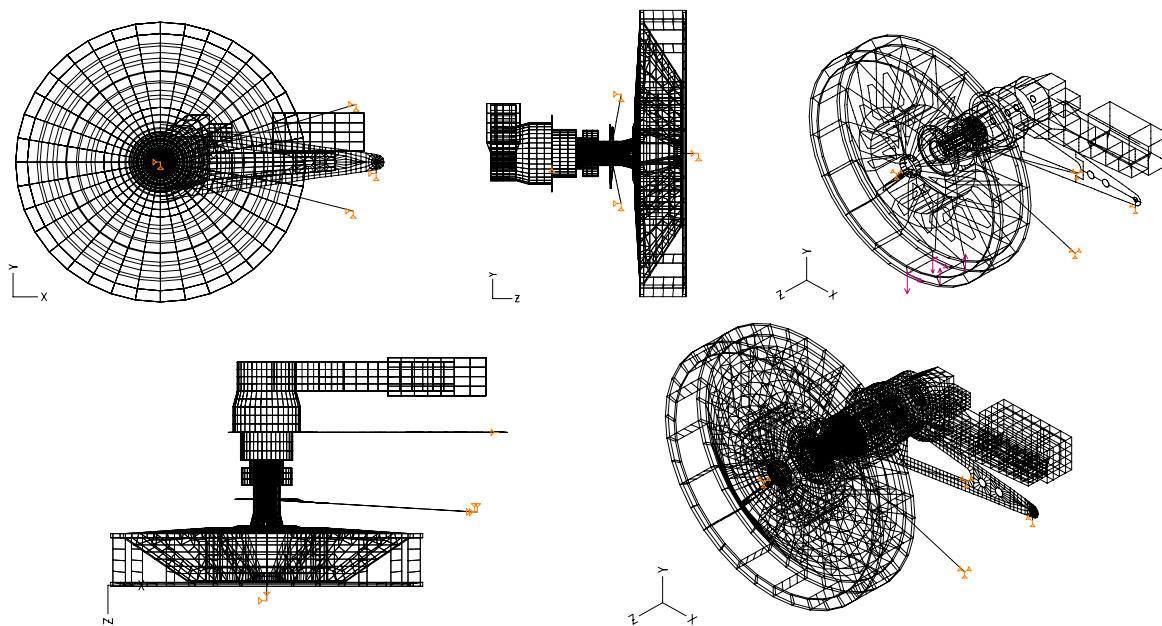
Računski model je generisan sa 6169 čvornih tačaka, odnosno 106 linijskih, 4355 površinskih i 1116 zapreminskih konačnih elemenata (sl. 29).

Successful exploitation of bucket requires the following parameters: low strain level (tooth oscillations in a cut are minimal); low stress and stress concentration level; presence of dominant normal and membrane stresses; low strain energy level of the bucket.

The presented diagnostics approach defines the necessary parameters the bucket must satisfy. It also defines the required reconstruction, i.e. the revitalisation of the bucket.

DIAGNOSTICS OF STATIC AND DYNAMIC BEHAVIOUR OF EXCAVATOR DIGGING SYSTEM SRS1300 KOSTOLAC-DRMNO

The computational model, generated with 6169 nodes, 106 linear, 4355 planar, and 1116 volume finite elements (Fig. 29).



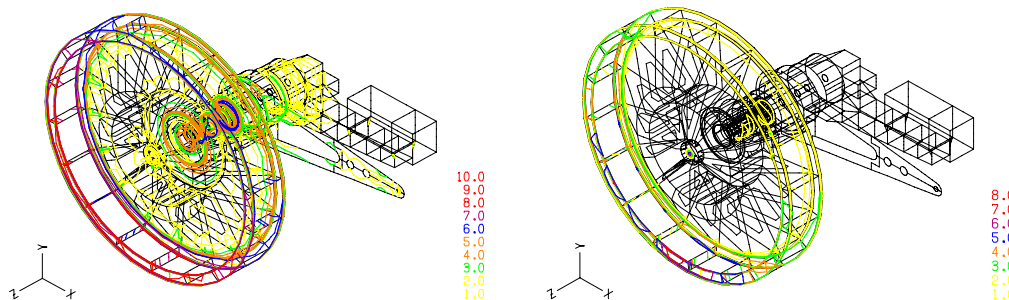
Slika 29. Geometrija računskog modela, statičko opterećenje i oslanjanje
Figure 29. Computational model geometry, static loads and supports.

Opterećenje sistema za kopanje predstavlja obrtni moment od 2 000 000 Nm, odnosno ukupni obimni otpor kopanja od 363 kN na $R = 4,5$ m. Ukupna bočna sila iznosi 134 kN.

Maksimalna deformacija sistema za kopanje pod zadatim opterećenjem iznosi 5,6 cm i odnosi se na uvijanje radnog točka. Naponsko polje i energija deformisanja sistema za kopanje prikazani su na sl. 30.

The digging system is loaded by a 2 000 000 Nm torque-turning moment, e.g. the total torque digging reaction is 363 kN at $R = 4.5$ m. The total lateral force is 134 kN.

Maximal deformation of the digging system under given load is 5.6 cm, and relates to torsion of the operating wheel. The stress field and strain energy of the digging system are shown in Fig. 30.



Slika 30. Raspodela napona [kN/cm²] i energije deformisanja [kNcm]
Figure 30. Stress [kN/cm²] and strain energy [kNcm] distribution.

Zaključak statičkog proračuna sistema za kopanje pri veoma visokom opterećenju glasi:

- deformacija konstrukcije je mala, prisutno je samo uvijanje radnog točka,
- nivo napona je nizak uz malu koncentraciju napona,
- najveći napon je na radnom točku,
- napon u elementima revitalizacije (šuplje vratilo, reduktor) je nizak.

Na sl. 31. prikazane su sopstvene oscilacije sistema za kopanje.

$f_{01} = 6.6$ Hz – poprečno savijanje momentne poluge (lateral bending of moment lever)

$f_{02} = 6.7$ Hz – uvijanje radnog točka (torsion of operating wheel)

$f_{03} = 7.5$ Hz – poprečno savijanje momentne poluge i reduktora (lateral bending of moment lever and transmission)

$f_{04} = 7.9$ Hz – savijanje radnog točka oko X ose i reduktora oko Z ose (bending of operating wheel – X axis, and transmission – Z axis)

$f_{05} = 9.2$ Hz – savijanje radnog točka oko Y ose i reduktora oko X ose (bending of operating wheel – Y axis, and transmission – X axis)

$f_{06} = 10$ Hz – savijanje radnog točka oko X ose i reduktora oko Z ose (bending of operating wheel – X axis, and transmission – Z axis)

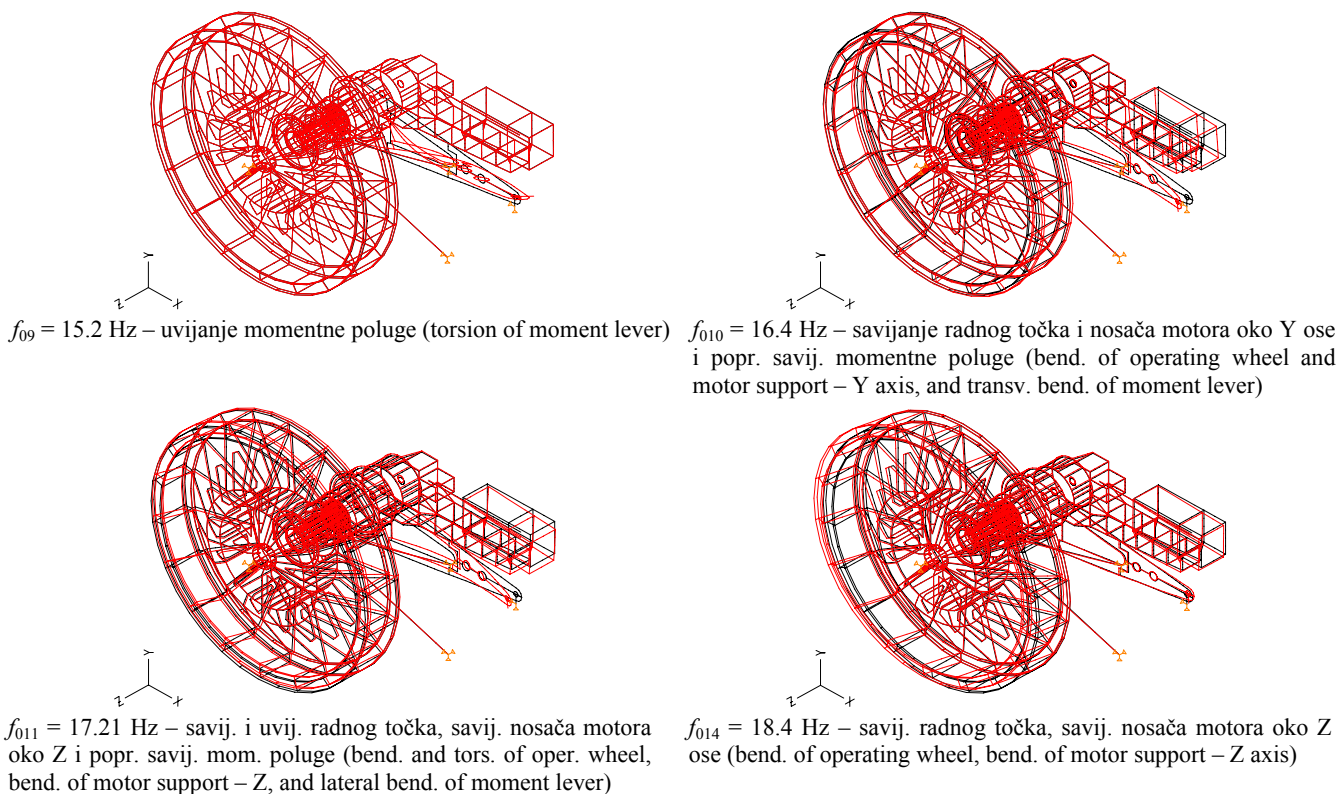
$f_{07} = 12.5$ Hz – uvijanje radnog točka i savijanje reduktora oko Z ose (torsion of operating wheel and bending of transmission – Z axis)

$f_{08} = 14.6$ Hz – savijanje radnog točka i reduktora oko Y ose i uvijanje poluge oko Y ose (bending of operating wheel and transmission. – Y axis, and torsion of moment lever - Y axis)

Static calculations of the digging system, at very high loads have drawn the following conclusions:

- strains in the structure are small, only torsion of the operating wheel is present,
- the stress level is low with small stress concentration,
- the largest stress is located on the operating wheel,
- the stress in revitalised elements (hollow shaft, transmission) is small.

Eigen-value frequencies of the digging system are shown in Fig. 31.



Slika 31. Glavni oblici oscilovanja sistema za kopanje
Figure 31. Main oscillation forms of the digging system.

Zaključak dinamičkog proračuna sistema za kopanje:

- nema korelacija sa frekvencijama kopanja,
- nema preloma vratila elektromotora i ulaznog vratila reduktora,
- u opsegu rada elektromotora postoji neznatno nepovoljno oscilovanje sa malim amplitudama momentne poluge i nosača elektromotora.

Conclusion of dynamic calculations of the digging system:

- no correlations to digging frequencies,
- no fractures of the electric motor and transmission entry shafts,
- in the operating range of the electric motor, insignificant negative oscillating occurs with small amplitudes in the moment lever and motor supports.

LITERATURA–REFERENCES

1. Maneski, T., *Kompjutersko modeliranje i proračun struktura*, Monografija, Mašinski fakultet, Beograd. (1998)
2. Maneski, T., *Rešeni problemi čvrstoće konstrukcija*, Mašinski fakultet, Beograd. (2002)
3. Maneski, T., Milošević-Mitić, V., Ostrić, D., *Postavke čvrstoće konstrukcija*, Mašinski fakultet, Beograd. (2002)
4. Ignjatović, D., Maneski, T. i saradnici., *Izvedeni projekti (performed projects)*